



Version 1.2

Theory Manual

Last Updated: October 19, 2010

Contributors

- Steve Maas (steve.maas@utah.edu)
- Dave Rawlins (rawlins@sci.utah.edu)
- Dr. Jeffrey Weiss (jeff.weiss@utah.edu)
- Dr. Gerard Ateshian (ateshian@columbia.edu)

Contact address

Musculoskeletal Research Laboratories, University of Utah
72 S. Central Campus Drive, Room 2646
Salt Lake City, Utah

Website

MRL: <http://mrl.sci.utah.edu>

FEBio: <http://mrl.sci.utah.edu/software/febio>

Forum

<http://mrlforums.sci.utah.edu/forums/>

Table of Contents

Table of Contents	2
Chapter 1. Introduction	4
1.1. Overview of FEBio	4
1.2. About this document	4
Chapter 2. Continuum Mechanics	6
2.1. Vectors and Tensors	6
2.2. The Directional Derivative	8
2.3. Deformation, Strain and Stress	9
2.3.1. The deformation gradient tensor	9
2.3.2. Strain	10
2.3.3. Stress	11
2.4. Hyperelasticity	12
2.4.1. Isotropic Hyperelasticity	12
2.4.2. Nearly-Incompressible Hyperelasticity	13
2.4.3. Transversely Isotropic Hyperelasticity	14
Chapter 3. The Nonlinear FE Method	16
3.1. Weak formulation	16
3.1.1. Linearization	16
3.1.2. Discretization	17
3.2. Newton-Raphson method	19
3.2.1. Full Newton Method	19
3.2.2. BFGS Method	20
3.2.3. Line Search Method	21
Chapter 4. Element Library	22
4.1. Solid Elements	22
4.1.1. Hexahedral elements	22
4.1.2. Pentahedral Elements	23
4.1.3. Tetrahedral Elements	23
4.2. Shell Elements	24
4.2.1. Shell formulation	25
4.2.2. Quadrilateral shells	26
4.2.3. Triangular shells	27
Chapter 5. Constitutive Models	28
5.1. Linear Elasticity	28
5.2. Isotropic Elasticity	30
5.3. Neo-Hookean Hyperelasticity	30
5.4. Mooney-Rivlin Hyperelasticity	30
5.5. Ogden Hyperelastic	31
5.6. Veronda-Westmann Hyperelasticity	31
5.7. Transversely Isotropic Hyperelastic	31
5.8. Biphasic Material	33
5.8.1. Governing Equations	33

5.8.2. Weak Formulation	34
5.8.3. Finite Element Equations	36
5.9. Active Contraction Model.....	39
Chapter 6. Contact and Coupling	40
6.1. Rigid-Deformable Coupling	40
6.1.1. Kinematics	40
6.1.2. A single rigid body.....	41
6.1.3. Multiple Rigid Bodies	42
6.2. Rigid Joints	42
6.3. Sliding Interfaces	43
6.3.1. Contact Kinematics	44
6.3.2. Weak Form of Two Body Contact.....	45
6.3.3. Linearization of the Contact Integral	46
6.3.4. Discretization of the Contact Integral	47
6.3.5. Discretization of the Contact Stiffness	48
6.3.6. Augmented Lagrangian Method	49
6.3.7. Automatic penalty calculation	50
6.3.8. Alternative formulations	50
6.4. Biphasic Contact	51
6.5. Tied Contact.....	52
6.5.1. Gap Function.....	52
6.5.2. Tied Contact Integral	52
6.5.3. Linearization of the Contact Integral	53
6.5.4. Discretization	53
References	55

Chapter 1. Introduction

1.1. Overview of FEBio

FEBio is an implicit, nonlinear finite element solver that is specifically designed for applications in biomechanics. It offers modeling scenarios, constitutive models and boundary conditions that are relevant for this particular field. This section describes the available features of FEBio.

FEBio supports two analysis types, namely *quasi-static* and *quasi-static poroelastic*. In a *quasi-static* analysis the (quasi-) static response of the system is sought; inertial terms are ignored. In a *quasi-static poroelastic* analysis a coupled solid-fluid problem is solved. The latter analysis type is useful for modeling tissues that have high water content and the explicit modeling of fluid movement relative to the solid phase is important.

Several nonlinear constitutive models are available to allow the user to model the often complicated biological tissue behavior. Several isotropic constitutive models are supported such as Neo-Hookean, Mooney-Rivlin, Veronda-Westmann, Arruda-Boyce and Ogden. These models have a nonlinear stress-strain response. In addition to the isotropic models, there are several anisotropic models available. These materials show anisotropic behavior in at least one preferred direction and are useful for modeling biological tissues such as tendons, muscles and other tissues that contain fibers. FEBio also contains a *rigid body* material model, which can be used to model rigid structures whose deformation is negligible compared to the deformable geometry.

Biological tissues can interact in very complicated ways. Therefore FEBio supports a wide range of boundary conditions to model these interactions. These include prescribed displacements, nodal forces, and pressure forces. Deformable models can also be connected to rigid bodies so that the user can model prescribed rotations and torques. Rigid bodies can be connected with rigid joints. Even more complicated interactions can be modeled using FEBio's contact interfaces. The user can choose between different types of contact interfaces, such as sliding interfaces, tied interfaces and rigid wall interfaces. A sliding interface is defined between two surfaces that are allowed to separate and slide across each other but are not allowed to penetrate. The rigid wall interface is also similar to the sliding interface, except that one of the contacting surfaces is a movable rigid wall. As of version 1.2, there is an implementation of a sliding interface that allows for fluid flow crossing the contact interface. The tied interface is similar to the sliding interface, but in this case, the surfaces are not allowed to slide or separate. In addition, the user may specify a body force which can be used to model the effects of gravity or base acceleration.

1.2. About this document

This document is a part of a set of three manuals that accompany FEBio: the [User's Manual](#), describing how to use FEBio, the [online](#) code documentation for users who wish

to modify or add features to the code, and this manual, which describes the theory behind most of the FEBio algorithms.

The purpose of this manual is to provide theoretical background on many of the algorithms that are implemented in FEBio. In this way the user can develop a better understanding of how the program works and how it can be used to create well defined biomechanical simulations. The authors have tried to be as detailed as possible to make the text coherent and comprehensible, but due to the complexity of some of the topics, some descriptions only skim the surface. Many of the theoretical ideas discussed in this manual can and have filled entire bookshelves. The explanations contained herein should be sufficient to give the reader a basic understanding of the theoretical developments. References to textbooks and the primary literature are provided for further reading.

Chapter 2 starts with a brief overview of some of the important concepts in continuum mechanics. Readers who are already familiar with this field can skip this chapter, although the material may be useful to get familiar with the notation and terminology used in this manual.

Chapter 3 describes the nonlinear finite element method. It also explains the Newton-Raphson method, which is the basis for most implementations of the nonlinear finite element method. A more specialized version of this algorithm, the BFGS method, is described as well since it is used in FEBio.

In Chapter 4 the different element types that are available in FEBio are described in detail. FEBio currently supports 3D solid elements, such as the linear hexahedral, pentahedral and tetrahedral elements, as well as quadrilateral and triangular shell elements.

Chapter 5 contains a detailed description of the material models in FEBio. Most of these models are based on hyperelasticity, which is introduced in chapter 2. Several transversely isotropic materials are described as well. This also discusses the biphasic material and its implementation in FEBio.

Chapter 6 describes the basics of the theory of contact and coupling. In FEBio the user can connect the different parts of the geometry in a variety of ways. There are rigid interfaces where a deformable model is attached to a rigid model, rigid joints where two or more rigid bodies connect, and sliding interfaces where two surfaces are allowed to separate and slide across each other but are not allowed to penetrate. The various contact and coupling algorithms are discussed as well together with their implementation in FEBio.

Chapter 2. Continuum Mechanics

This chapter contains an overview of some of the important concepts from continuum mechanics and establishes some of the notation and terminology that will be used in the rest of this document. The section begins by introducing the important concepts of deformation, stress and strain. Next the concept of hyperelasticity is discussed. Finally the concept of virtual work is discussed. This concept will be used later to derive the nonlinear finite element equations. For a more thorough introduction to the mathematics needed for continuum mechanics, the user can consult [1].

2.1. Vectors and Tensors

It is assumed that the reader is familiar with the concepts of vectors and tensors. This section summarizes the notation and some useful relations that will be used throughout the manual.

Vectors are denoted by small, bold letters, e.g. \mathbf{v} . Their components will be denoted by v_i , where, unless otherwise stated, Latin under scripts such as i or I will range from 1 to 3. In matrix form a vector will be represented as a column vector and its transpose as a row vector:

$$\mathbf{v} = \begin{pmatrix} v_1 \\ v_2 \\ v_3 \end{pmatrix}, \quad \mathbf{v}^T = v_1, \quad v_2, \quad v_3. \quad (2.1)$$

The following products are defined between vectors. Assume \mathbf{u} , \mathbf{v} are vectors. Also note that we use the Einstein summation convention throughout this manual.

The *dot* or *scalar product*:

$$\mathbf{u} \cdot \mathbf{v} = u_i v_i. \quad (2.2)$$

The *vector* or *cross product*:

$$\mathbf{u} \times \mathbf{v} = \begin{bmatrix} u_2 v_3 - u_3 v_2 \\ u_3 v_1 - u_1 v_3 \\ u_1 v_2 - u_2 v_1 \end{bmatrix}. \quad (2.3)$$

The *outer product*:

$$\mathbf{u} \otimes \mathbf{v}_{ij} = u_i v_j. \quad (2.4)$$

Note that vectors are also known as first order tensors. Scalars are known as zero order tensors. The outer product, defined by equation (2.4), is a second order tensor.

Second order tensors are denoted by bold, capital letters, e.g. \mathbf{A} . Some exceptions will be made to remain consistent with the current literature. For instance, the Cauchy stress tensor is denoted by $\boldsymbol{\sigma}$. However, the nature of the objects will always be clear from the context. The following operations on tensors are defined. Assume \mathbf{A} and \mathbf{B} are second-order tensors.

The *double contraction*, or *tensor inner product* is defined as:

$$\mathbf{A} : \mathbf{B} = A_{ij} B_{ij} . \quad (2.5)$$

The *trace* is defined as:

$$\text{tr } \mathbf{A} = \mathbf{1} : \mathbf{A} = A_{ii} . \quad (2.6)$$

Here $\mathbf{1}$ is the second order identity tensor.

In general the components of tensors will change under a change of coordinate system. Nevertheless, certain intrinsic quantities associated with them will remain invariant under such a transformation. The scalar product between two vectors is such an example. The double contraction between two second-order tensors is another example. The following set of invariants for second-order tensors is commonly used:

$$\begin{aligned} I_1 &= \text{tr } \mathbf{A} \\ I_2 &= \frac{1}{2} \text{tr } \mathbf{A}^2 - \text{tr } \mathbf{A}^2 . \\ I_3 &= \det \mathbf{A} \end{aligned} \quad (2.7)$$

A tensor \mathbf{S} is called symmetric if it is equal to its transpose:

$$\mathbf{S} = \mathbf{S}^T . \quad (2.8)$$

A tensor \mathbf{W} is called anti-symmetric if it is equal to the negative of its transpose:

$$\mathbf{W} = -\mathbf{W}^T . \quad (2.9)$$

Any second order tensor \mathbf{A} can be written as the sum of a symmetric tensor \mathbf{S} and an anti-symmetric tensor \mathbf{W} :

$$\mathbf{A} = \mathbf{S} + \mathbf{W} , \quad (2.10)$$

where

$$\begin{aligned} \mathbf{S} &= \frac{1}{2} (\mathbf{A} + \mathbf{A}^T) \\ \mathbf{W} &= \frac{1}{2} (\mathbf{A} - \mathbf{A}^T) . \end{aligned} \quad (2.11)$$

Also note that for any tensor \mathbf{B} the following holds:

$$\mathbf{B} : \mathbf{A} = \mathbf{B} : \mathbf{S}, \quad \mathbf{B} : \mathbf{W} = \mathbf{0} . \quad (2.12)$$

With any anti-symmetric tensor a vector \mathbf{w} can be associated such that,

$$\hat{\mathbf{w}} \mathbf{u} = \mathbf{w} \times \mathbf{u} , \quad (2.13)$$

where the second order tensor $\hat{\mathbf{w}}$ is defined as,

$$\hat{\mathbf{w}} = \begin{bmatrix} 0 & -w_3 & w_2 \\ w_3 & 0 & -w_1 \\ -w_2 & w_1 & 0 \end{bmatrix} . \quad (2.14)$$

A second order \mathbf{Q} tensor is called *orthogonal* if $\mathbf{Q}^{-1} = \mathbf{Q}^T$. For such tensors, the inverse tensor equals its transposed.

In the implementation of the FE method it is often convenient to write symmetric second-order tensors using *Voigt notation*. In this notation the components of a 2nd order symmetric tensor \mathbf{A} are arranged as a column vector:

$$\underline{\mathbf{A}} = \begin{bmatrix} A_{11} \\ A_{22} \\ A_{33} \\ A_{12} \\ A_{23} \\ A_{13} \end{bmatrix}. \quad (2.15)$$

Higher order tensors will be denoted by bold, capital, script symbols, e.g. \mathcal{A} . An example of a third-order tensor is the *permutation tensor* \mathcal{E} , whose components are 1 for an even permutation of 1,2,3, -1 for an odd permutation of 1,2,3 and zero otherwise. The permutation symbol is useful for expressing the cross-product of two vectors in index notation.

$$\mathbf{u} \times \mathbf{v} \quad_i = \mathcal{E}_{ijk} u_j v_k \quad (2.16)$$

An example of a fourth order tensor is the elasticity tensor \mathcal{C} which, in linear elasticity theory, relates the small strain tensor $\boldsymbol{\varepsilon}$ and the Cauchy stress tensor $\boldsymbol{\sigma} = \mathcal{C} : \boldsymbol{\varepsilon}$.

2.2. The Directional Derivative

In later sections the nonlinear finite element method will be formulated. Anticipating an iterative solution method to solve the nonlinear equations, it will be necessary to linearize the quantities involved. This linearization process will utilize a construction called the *directional derivative* [1] which we shall introduce briefly here.

The directional derivative of a function $f(\mathbf{x})$ is defined as follows:

$$Df(\mathbf{x}) \cdot \mathbf{u} = \left. \frac{d}{d\varepsilon} \right|_{\varepsilon=0} f(\mathbf{x} + \varepsilon \mathbf{u}). \quad (2.17)$$

The quantity \mathbf{x} may be a scalar, a vector or even a vector of unknown functions. For instance, consider a scalar function $f(\mathbf{x})$, where \mathbf{x} is the position vector in \mathbb{R}^3 . In this case the directional derivative is given by>

$$\begin{aligned} Df(\mathbf{x}) \cdot \mathbf{u} &= \left. \frac{d}{d\varepsilon} \right|_{\varepsilon=0} f(\mathbf{x} + \varepsilon \mathbf{u}) \\ &= \frac{\partial f}{\partial x_i} u_i \\ &= \nabla f \cdot \mathbf{u} \end{aligned} \quad (2.18)$$

Here, the symbol ∇ (“del”) depicts the familiar gradient operator.

The linearization of a function implies that it is approximated by a linear function. Using the directional derivative a function f can be linearized as follows:

$$f(\mathbf{x} + \mathbf{u}) \cong f(\mathbf{x}) + Df(\mathbf{x}) \cdot \mathbf{u} . \quad (2.19)$$

The directional derivative obeys the usual properties for derivatives.

(a) *sum rule*: If $f = f_1 + f_2$, then

$$Df(\mathbf{x}) \cdot \mathbf{u} = Df_1(\mathbf{x}) \cdot \mathbf{u} + Df_2(\mathbf{x}) \cdot \mathbf{u} . \quad (2.20)$$

(b) *product rule*: If $f = f_1 \cdot f_2$, then

$$Df(\mathbf{x}) \cdot \mathbf{u} = f_1(\mathbf{x}) \cdot Df_2(\mathbf{x}) \cdot \mathbf{u} + f_2(\mathbf{x}) \cdot Df_1(\mathbf{x}) \cdot \mathbf{u} . \quad (2.21)$$

(c) *chain rule*: If $f = g \circ h(\mathbf{x})$, then

$$Df(\mathbf{x}) \cdot \mathbf{u} = Dg(h(\mathbf{x})) \cdot [Dh(\mathbf{x}) \cdot \mathbf{u}] . \quad (2.22)$$

2.3. Deformation, Strain and Stress

2.3.1. The deformation gradient tensor

Consider the deformation of an object when it moves from the initial or *reference configuration* to the *current configuration*. The location of the material particles in the reference configuration are denoted by \mathbf{X} and are known as the *material coordinates*. Their location in the current configuration is denoted by \mathbf{x} and known as the *spatial coordinates*. The *deformation map* φ , which is a mapping from \mathbb{R}^3 to \mathbb{R}^3 , maps the coordinates of a material point to the spatial configuration:

$$\mathbf{x} = \varphi(\mathbf{X}) . \quad (2.23)$$

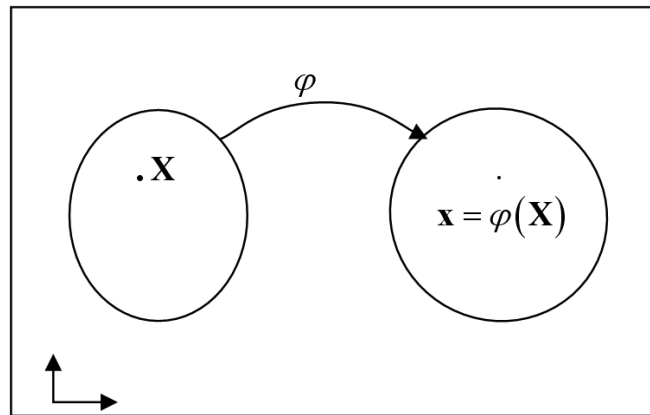


Figure 2-1. The deformation map

The displacement map \mathbf{u} is defined as the difference between the spatial and material coordinates:

$$\mathbf{x} = \mathbf{X} + \mathbf{u}(\mathbf{X}) . \quad (2.24)$$

The *deformation gradient tensor* is defined as

$$\mathbf{F} = \frac{\partial \varphi}{\partial \mathbf{X}} . \quad (2.25)$$

This tensor relates an infinitesimal vector in the reference configuration $d\mathbf{X}$ to the corresponding vector in the current configuration:

$$d\mathbf{x} = \mathbf{F} \cdot d\mathbf{X} . \quad (2.26)$$

The determinant of the deformation tensor $J = \det \mathbf{F}$ gives the volume change, or equivalently the change in density:

$$\rho_0 = \rho J . \quad (2.27)$$

Here ρ_0 is the density in the reference configuration and ρ is the current density.

When dealing with incompressible and nearly incompressible materials it will prove useful to separate the volumetric and the deviatoric (distortional) components of the deformation gradient. Such a separation must ensure that the deviatoric component, namely $\tilde{\mathbf{F}}$, does not produce any change in volume. Noting that the determinant of the deformation gradient gives the volume ratio, the determinant of $\tilde{\mathbf{F}}$ must therefore satisfy,

$$\det \tilde{\mathbf{F}} = 1 . \quad (2.28)$$

This condition can be achieved by choosing $\tilde{\mathbf{F}}$ as,

$$\tilde{\mathbf{F}} = J^{-1/3} \mathbf{F} . \quad (2.29)$$

Using the polar decomposition of a second order tensor, the deformation gradient can be written as a product of a symmetric tensor \mathbf{U} and an orthogonal tensor \mathbf{Q} :

$$\mathbf{F} = \mathbf{U} \mathbf{Q} . \quad (2.30)$$

The symmetric tensor \mathbf{U} is called the (*left*) *stretch tensor* and the orthogonal tensor \mathbf{Q} is called the *rotation tensor*.

2.3.2. Strain

The *right Cauchy-Green deformation tensor* is defined as follows:

$$\mathbf{C} = \mathbf{F}^T \mathbf{F} . \quad (2.31)$$

This tensor is an example of a *material tensor* and is a function of the material coordinates \mathbf{X} . The *left Cauchy-Green deformation tensor* is defined as follows:

$$\mathbf{B} = \mathbf{F} \mathbf{F}^T . \quad (2.32)$$

This tensor is an example of a *spatial tensor* and is a function of the spatial coordinates \mathbf{x} . The implementation of the updated Lagrangian finite element method used by FEBio is described in the spatial configuration.

The left and right deformation tensors can also be split into volumetric and deviatoric components. With the use of (2.29), the deviatoric deformation tensors are:

$$\begin{aligned} \tilde{\mathbf{C}} &= \tilde{\mathbf{F}}^T \tilde{\mathbf{F}} = J^{-2/3} \mathbf{C} \\ \tilde{\mathbf{B}} &= \tilde{\mathbf{F}} \tilde{\mathbf{F}}^T = J^{-2/3} \mathbf{B} \end{aligned} \quad (2.33)$$

The deformation tensors defined above are not good candidates for strain measures since in the absence of strain they become the unity tensor $\mathbf{1}$ $\mathbf{1}_{ij} = \delta_{ij}$. However, they can be used to define strain measures. The *Green-Lagrange strain tensor* is defined as:

$$\mathbf{E} = \frac{1}{2} (\mathbf{C} - \mathbf{1}) . \quad (2.34)$$

This tensor is a material tensor. Its spatial equivalent is known as the *Almansi strain tensor* and is defined as:

$$\mathbf{e} = \frac{1}{2} \mathbf{1} - \mathbf{B}^{-1} . \quad (2.35)$$

In the limit of small displacement gradients, the components of both strain tensors are identical, resulting in the *small strain tensor* or *infinitesimal strain tensor*:

$$\boldsymbol{\varepsilon} = \frac{1}{2} \left(\frac{\partial \mathbf{u}}{\partial \mathbf{x}} + \left(\frac{\partial \mathbf{u}}{\partial \mathbf{x}} \right)^T \right) . \quad (2.36)$$

Note that the small strain tensor is also the linearization of the Green Lagrange strain,

$$DE \mathbf{u} = \mathbf{F}^T \boldsymbol{\varepsilon} \mathbf{F} . \quad (2.37)$$

2.3.3. Stress

The traction \mathbf{t} on a plane bisecting the body is given by,

$$\mathbf{t} = \boldsymbol{\sigma} \cdot \mathbf{n} , \quad (2.38)$$

where $\boldsymbol{\sigma}$ is the *Cauchy stress tensor* and \mathbf{n} is the outward unit normal vector to the plane. It can be shown that by the conservation of angular momentum that this tensor is symmetric ($\sigma_{ij} = \sigma_{ji}$) [2]. The Cauchy stress tensor, a spatial tensor, is the actual physical stress, that is, the force per unit deformed area. To simplify the equations of continuum mechanics, especially when working in the material configuration, several other stress measures are available. The *Kirchhoff stress tensor* is defined as

$$\boldsymbol{\tau} = J \boldsymbol{\sigma} . \quad (2.39)$$

The *first Piola-Kirchhoff stress tensor* is given as

$$\mathbf{P} = J \boldsymbol{\sigma} \mathbf{F}^{-T} . \quad (2.40)$$

Note that \mathbf{P} , like \mathbf{F} , is not symmetric. Also, like \mathbf{F} , \mathbf{P} is known as a *two-point* tensor, meaning it is neither a material nor a spatial tensor. Since we have two strain tensors, one spatial and one material tensor, it would be useful to have similar stress measures. The Cauchy stress is a spatial tensor and the *second Piola-Kirchhoff (2nd PK) stress tensor*, defined as

$$\mathbf{S} = J \mathbf{F}^{-1} \boldsymbol{\sigma} \mathbf{F}^{-T} , \quad (2.41)$$

is a material tensor. The inverse relations are:

$$\boldsymbol{\sigma} = \frac{1}{J} \boldsymbol{\tau}, \quad \boldsymbol{\sigma} = \frac{1}{J} \mathbf{P} \mathbf{F}^T, \quad \boldsymbol{\sigma} = \frac{1}{J} \mathbf{F} \mathbf{S} \mathbf{F}^T . \quad (2.42)$$

In many practical applications it is physically relevant to separate the hydrostatic stress and the deviatoric stress $\tilde{\boldsymbol{\sigma}}$ of the Cauchy stress tensor.

$$\boldsymbol{\sigma} = \tilde{\boldsymbol{\sigma}} + p \mathbf{1} \quad (2.43)$$

Here, the pressure is defined as $p = \frac{1}{3} \text{tr} \boldsymbol{\sigma}$. Note that the deviatoric Cauchy stress tensor satisfies $\text{tr} \tilde{\boldsymbol{\sigma}} = 0$.

In the linearization of the finite element equations the directional derivative of the 2nd PK stress tensor needs to be calculated. For a hyperelastic material, a linear relationship between the directional derivative of \mathbf{S} and the linearized strain $DE \mathbf{u}$ can be obtained:

$$DS \mathbf{u} = \mathcal{C} : DE \mathbf{u} . \quad (2.44)$$

Here, \mathcal{C} is a fourth-order tensor known as the *material elasticity tensor*. Its components are given by,

$$\mathcal{C}_{IJKL} = \frac{\partial S_{IJ}}{\partial E_{KL}} = \frac{4\partial^2 \Psi}{\partial C_{IJ} \partial C_{KL}}, \quad (2.45)$$

where Ψ is the strain-energy density function for the hyperelastic material. The spatial equivalent – the *spatial elasticity tensor* – can be obtained by,

$$\mathcal{C}_{ijkl} = \frac{1}{J} F_{iI} F_{jJ} F_{kK} F_{lL} \mathcal{C}_{IJKL}. \quad (2.46)$$

2.4. Hyperelasticity

When the constitutive behavior is only a function of the current state of deformation, the material is *elastic*. In the special case when the work done by the stresses during a deformation is only dependent on the initial state and the final state, the material is termed *hyperelastic* and its behavior is path-independent. As a consequence of the path-independence a *strain energy function* per unit undeformed volume can be defined as the work done by the stresses from the initial to the final configuration:

$$\Psi(\mathbf{F}, \mathbf{X}) = \int_{t_0}^t \mathbf{P}(\mathbf{F}, \mathbf{X}) : \dot{\mathbf{F}} dt. \quad (2.47)$$

The rate of change of the potential is then given by

$$\dot{\Psi}(\mathbf{F}, \mathbf{X}) = \mathbf{P} : \dot{\mathbf{F}}. \quad (2.48)$$

Or alternatively,

$$P_{iJ} = \sum_{i,J=1}^3 \frac{\partial \Psi}{\partial F_{iJ}} \dot{F}_{iJ}. \quad (2.49)$$

Comparing (2.48) with (2.49) reveals that

$$\mathbf{P}(\mathbf{F}, \mathbf{X}) = \frac{\partial \Psi(\mathbf{F}, \mathbf{X})}{\partial \mathbf{F}}. \quad (2.50)$$

This general constitutive equation can be further developed by observing that, as a consequence of the objectivity requirement, Ψ may only depend on \mathbf{F} through the stretch tensor \mathbf{U} and must be independent of the rotation component \mathbf{R} . For convenience,

however, Ψ is often expressed as a function of $\mathbf{C} = \mathbf{U}^2 = \mathbf{F}^T \mathbf{F}$. Noting that $\frac{1}{2} \dot{\mathbf{C}} = \dot{\mathbf{E}}$ is work conjugate to the second Piola-Kirchhoff stress \mathbf{S} , establishes the following general relationships for hyperelastic materials:

$$\dot{\Psi} = \frac{\partial \Psi}{\partial \mathbf{C}} : \dot{\mathbf{C}} = \frac{1}{2} \mathbf{S} : \dot{\mathbf{C}}, \quad \boxed{\mathbf{S}(\mathbf{C}, \mathbf{X}) = 2 \frac{\partial \Psi}{\partial \mathbf{C}} = \frac{\partial \Psi}{\partial \mathbf{E}}}. \quad (2.51)$$

2.4.1. Isotropic Hyperelasticity

The hyperelastic constitutive equations discussed so far are unrestricted in their application. Isotropic material symmetry is defined by requiring the constitutive behavior to be independent of the material axis chosen and, consequently, Ψ must only be a function of the invariants of \mathbf{C} ,

$$\Psi(\mathbf{C}, \mathbf{X}) = \Psi(I_1, I_2, I_3, \mathbf{X}), \quad (2.52)$$

where the invariants of \mathbf{C} are defined here as,

$$\begin{aligned} I_1 &= \text{tr } \mathbf{C} = \mathbf{C} : \mathbf{1} \\ I_2 &= \frac{1}{2} \left[\text{tr } \mathbf{C}^2 - \text{tr } \mathbf{C}^2 \right]. \\ I_3 &= \det \mathbf{C} = J^2 \end{aligned} \quad (2.53)$$

As a result of the isotropic restriction, the second Piola-Kirchhoff stress tensor can be written as,

$$\mathbf{S} = 2 \frac{\partial \Psi}{\partial \mathbf{C}} = 2 \frac{\partial \Psi}{\partial I_1} \frac{\partial I_1}{\partial \mathbf{C}} + 2 \frac{\partial \Psi}{\partial I_2} \frac{\partial I_2}{\partial \mathbf{C}} + 2 \frac{\partial \Psi}{\partial I_3} \frac{\partial I_3}{\partial \mathbf{C}}. \quad (2.54)$$

The second order tensors formed by the derivatives of the invariants with respect to \mathbf{C} can be evaluated as follows:

$$\begin{aligned} \frac{\partial I_1}{\partial \mathbf{C}} &= \mathbf{1}, \\ \frac{\partial I_2}{\partial \mathbf{C}} &= I_1 \mathbf{1} - \mathbf{C}, \\ \frac{\partial I_3}{\partial \mathbf{C}} &= I_3 \mathbf{C}^{-1}. \end{aligned} \quad (2.55)$$

Introducing expressions (2.55) into equation (2.54) enables the second Piola-Kirchhoff stress to be evaluated as,

$$\mathbf{S} = 2 \left(\Psi_1 + I_1 \Psi_2 + I_2 \Psi_3 \right) \mathbf{1} - \Psi_2 + I_1 \Psi_3 \mathbf{C} + \Psi_3 \mathbf{C}^2, \quad (2.56)$$

where $\Psi_1 = \partial \Psi / \partial I_1$, $\Psi_2 = \partial \Psi / \partial I_2$, and $\Psi_3 = \partial \Psi / \partial I_3$.

The Cauchy stresses can now be obtained indirectly from the second Piola-Kirchhoff stresses by using (2.42):

$$\boldsymbol{\sigma} = 2 \left(\Psi_1 + I_1 \Psi_2 + I_2 \Psi_3 \right) \mathbf{B} - \Psi_2 + I_1 \Psi_3 \mathbf{B}^2 + \Psi_3 \mathbf{B}^3. \quad (2.57)$$

Note that in this equation Ψ_1 , Ψ_2 , and Ψ_3 still involve derivatives with respect to the invariants of \mathbf{C} . However, since the invariants of \mathbf{B} are identical to those of \mathbf{C} , the quantities Ψ_1 , Ψ_2 and Ψ_3 may also be considered to be the derivatives with respect to the invariants of \mathbf{B} .

2.4.2. Nearly-Incompressible Hyperelasticity

A material is considered incompressible if it shows no change in volume during deformation, or otherwise stated if $J = 1$ holds throughout the entire body. It can be shown [1] that if the material is incompressible the hyperelastic constitutive equation becomes

$$\mathbf{S} = 2 \frac{\partial \tilde{\Psi}}{\partial \mathbf{C}} + p J \mathbf{C}^{-1}, \quad (2.58)$$

where $\tilde{\Psi} = \Psi - \tilde{C}$ is the deviatoric strain energy function and p is the hydrostatic pressure. The presence of J may seem unnecessary, but retaining J has the advantage that equation (2.58) remains valid in the nearly incompressible case. Further, in practical terms, a finite element analysis rarely enforces $J = 1$ in a pointwise manner, and hence its retention may be important for the evaluation of stresses.

The process of defining constitutive equations in the case of nearly incompressible hyperelasticity is simplified by adding a volumetric energy component $U(J)$ to the distortional component $\tilde{\Psi}(\mathbf{C})$:

$$\Psi(\mathbf{C}) = \tilde{\Psi}(\mathbf{C}) + U(J). \quad (2.59)$$

The second Piola-Kirchhoff tensor for a material defined by (2.59) is obtained in the standard manner with the help of equation (2.54).

$$\begin{aligned} \mathbf{S} &= 2 \frac{\partial \Psi}{\partial \mathbf{C}} \\ &= 2 \frac{\partial \tilde{\Psi}}{\partial \mathbf{C}} + 2 \frac{dU}{dJ} \frac{\partial J}{\partial \mathbf{C}} \\ &= 2 \frac{\partial \tilde{\Psi}}{\partial \mathbf{C}} + p J \mathbf{C}^{-1}, \end{aligned} \quad (2.60)$$

where the pressure is defined as

$$p = \frac{dU}{dJ}. \quad (2.61)$$

An example for U that will be used later in the definition of the constitutive models is

$$U(J) = \frac{1}{2} \kappa (\ln J)^2. \quad (2.62)$$

The parameter κ will be used later as a penalty factor that will enforce the (nearly-) incompressible constraint. However, κ can represent a true material coefficient, namely the bulk modulus, for a compressible material that happens to have a hyperelastic strain energy function in the form of (2.59). In the case where the dilatational energy is given by (2.62) the pressure is

$$p = \kappa \frac{\ln J}{J}. \quad (2.63)$$

2.4.3. Transversely Isotropic Hyperelasticity

Transverse isotropy can be introduced by adding a vector field representing the material preferred direction explicitly into the strain energy [3]. We require that the strain energy depends on a unit vector field \mathbf{a}^0 , which describes the local fiber direction in the undeformed configuration. When the material undergoes deformation, the vector $\mathbf{a}^0 \cdot \mathbf{X}$ may be described by a unit vector field $\mathbf{a}(\boldsymbol{\varphi}, \mathbf{X})$. In general, the fibers will also undergo length change. The fiber stretch, λ , can be determined in terms of the deformation gradient and the fiber direction in the undeformed configuration,

$$\lambda \mathbf{a} = \mathbf{F} \cdot \mathbf{a}^0. \quad (2.64)$$

Also, since \mathbf{a} is a unit vector,

$$\lambda^2 = \mathbf{a}^0 \cdot \mathbf{C} \cdot \mathbf{a}^0. \quad (2.65)$$

The strain energy function for a transversely isotropic material, $\Psi(\mathbf{C}, \mathbf{a}^0, \mathbf{X})$ is an isotropic function of \mathbf{C} and $\mathbf{a}^0 \otimes \mathbf{a}^0$. It can be shown [2] that the following set of invariants are sufficient to describe the material fully:

$$I_1 = \text{tr} \mathbf{C}, \quad I_2 = \frac{1}{2} \left[\text{tr} \mathbf{C}^2 - \text{tr} \mathbf{C}^2 \right], \quad I_3 = \det \mathbf{C} = J^2, \quad (2.66)$$

$$I_4 = \mathbf{a}^0 \cdot \mathbf{C} \cdot \mathbf{a}^0, \quad I_5 = \mathbf{a}^0 \cdot \mathbf{C}^2 \cdot \mathbf{a}^0. \quad (2.67)$$

The strain energy function can be written in terms of these invariants such that

$$\Psi(\mathbf{C}, \mathbf{a}^0, \mathbf{X}) = \Psi(I_1, I_2, I_3, I_4, I_5, \mathbf{C}, \mathbf{a}^0). \quad (2.68)$$

The second Piola-Kirchhoff can now be obtained in the standard manner:

$$\mathbf{S} = 2 \frac{\partial \Psi}{\partial \mathbf{C}} = 2 \sum_{i=1}^5 \frac{\partial \Psi}{\partial I_i} \frac{\partial I_i}{\partial \mathbf{C}}. \quad (2.69)$$

In the transversely isotropic constitutive models described in Chapter 5 it is further assumed that the strain energy function can be split into the following terms:

$$\Psi(\mathbf{C}, \mathbf{a}^0) = \Psi_1(I_1, I_2, I_3) + \Psi_2(I_4) + \Psi_3(I_1, I_2, I_3, I_4). \quad (2.70)$$

The strain energy function Ψ_1 represents the material response of the isotropic ground substance matrix, Ψ_2 represents the contribution from the fiber family (e.g. collagen), and Ψ_3 is the contribution from interactions between the fibers and matrix. The form (2.70) generalizes many constitutive equations that have been successfully used in the past to describe biological soft tissues e.g. [4-6]. While this relation represents a large simplification when compared to the general case, it also embodies almost all of the material behavior that one would expect from transversely isotropic, large deformation matrix-fiber composites.

Chapter 3. The Nonlinear FE Method

This chapter discusses the basic principles of the nonlinear finite element method. The chapter begins with a short introduction to the weak formulation and the principle of virtual work. Next, the important concept of linearization is discussed and applied to the principle of virtual work. Finally the Newton-Raphson procedure and its application to the nonlinear finite element method are described.

3.1. Weak formulation

Generally, the finite element formulation is established in terms of a weak form of the differential equations under consideration. In the context of solid mechanics this implies the use of the virtual work equation:

$$\delta W = \int_V \boldsymbol{\sigma} : \delta \mathbf{d} dv - \int_V \mathbf{f} \cdot \delta \mathbf{v} dv - \int_{\partial V} \mathbf{t} \cdot \delta \mathbf{v} da = 0. \quad (3.1)$$

Here, $\delta \mathbf{v}$ is a virtual velocity and $\delta \mathbf{d}$ is the virtual rate of deformation tensor. This equation is known as the *spatial virtual work equation* since it is formulated using spatial quantities only. We can also define the *material virtual work equation* by expressing the principle of virtual work using only material quantities.

$$\delta W = \int_V \mathbf{S} : \delta \dot{\mathbf{E}} dV - \int_V \mathbf{f}_0 \cdot \delta \mathbf{v} dV - \int_{\partial V} \mathbf{t}_0 \cdot \delta \mathbf{v} dA = 0 \quad (3.2)$$

Here, $\mathbf{f}_0 = \mathbf{J}\mathbf{f}$ is the body force per unit undeformed volume and $\mathbf{t}_0 = \mathbf{t} da/dA$ is the traction vector per unit initial area.

3.1.1. Linearization

Equation (3.1) is the starting point for the nonlinear finite element method. It is highly nonlinear and any method attempting to solve this equation, such as the Newton-Raphson method, necessarily has to be iterative.

To linearize the finite element equations, the directional derivative of the virtual work in equation (3.1) must be calculated. In an iterative procedure, the quantity ϕ will be approximated by a trial solution ϕ_k . Linearization of the virtual work equation around this trial solution gives

$$\delta W_{\phi_k, \delta \mathbf{v}} + D\delta W_{\phi_k, \delta \mathbf{v}} \mathbf{u} = 0. \quad (3.3)$$

The directional derivative of the virtual work will eventually lead to the definition of the stiffness matrix. In order to proceed, it is convenient to split the virtual work into an internal and external virtual work component:

$$D\delta W_{\phi, \delta \mathbf{v}} \mathbf{u} = D\delta W_{\text{int}} \phi, \delta \mathbf{v} \mathbf{u} - D\delta W_{\text{ext}} \phi, \delta \mathbf{v} \mathbf{u}, \quad (3.4)$$

where

$$\delta W_{\text{int}} \phi, \delta \mathbf{v} = \int_V \boldsymbol{\sigma} : \delta \mathbf{d} dv, \quad (3.5)$$

and

$$\delta W_{\text{ext}} \phi, \delta \mathbf{v} = \int_V \mathbf{f} \cdot \delta \mathbf{v} dv + \int_{\partial V} \mathbf{t} \cdot \delta \mathbf{v} da. \quad (3.6)$$

The result is listed here without details of the derivation – see [1] for details. The linearization of the internal virtual work is given by

$$D\delta W_{\text{int}} \phi, \delta \mathbf{v} \mathbf{u} = \int_V \delta \mathbf{d} : \mathbf{C} : \varepsilon dv + \int_V \boldsymbol{\sigma} : \left[\nabla \mathbf{u}^T \nabla \delta \mathbf{v} \right] dv. \quad (3.7)$$

Notice that this equation is symmetric in $\delta \mathbf{v}$ and \mathbf{u} . This symmetry will, upon discretization, yield a symmetric tangent matrix.

The external virtual work has contributions from both body forces and surface tractions. The precise form of the linearized external virtual work depends on the form of these forces. FEBio currently supports gravity as a body force, $\mathbf{f} = \rho \mathbf{g}$. Since this force is independent of the geometry, the contribution to the linearized external work is zero. For surface tractions, normal pressure forces may be represented in FEBio. The linearized external work for this type of traction is given by

$$\begin{aligned} D\delta W_{\text{ext}}^p \phi, \delta \mathbf{v} \mathbf{u} = & \frac{1}{2} \int_{A_\xi} p \frac{\partial \mathbf{x}}{\partial \xi} \cdot \left[\left(\frac{\partial \mathbf{u}}{\partial \eta} \times \delta \mathbf{v} \right) + \left(\frac{\partial \delta \mathbf{v}}{\partial \eta} \times \mathbf{u} \right) \right] d\xi d\eta \\ & - \frac{1}{2} \int_{A_\xi} p \frac{\partial \mathbf{x}}{\partial \eta} \cdot \left[\left(\frac{\partial \mathbf{u}}{\partial \xi} \times \delta \mathbf{v} \right) + \left(\frac{\partial \delta \mathbf{v}}{\partial \xi} \times \mathbf{u} \right) \right] d\xi d\eta. \end{aligned} \quad (3.8)$$

Discretization of this equation will also lead to a symmetric component of the tangent matrix.

3.1.2. Discretization

The basis of the finite element method is that the domain of the problem (that is, the volume of the object under consideration) is divided into smaller subunits, called *finite elements*. In the case of *isoparametric elements* it is further assumed that each element has a local coordinate system, named the *natural coordinates*, and the coordinates and shape of the element are discretized using the same functions. The discretization process is established by interpolating the geometry in terms of the coordinates \mathbf{X}_a of the *nodes* that define the geometry of a finite element, and the *shape functions*:

$$\mathbf{X} = \sum_{a=1}^n N_a \xi_1, \xi_2, \xi_3 \mathbf{X}_a, \quad (3.9)$$

where n is the number of nodes and ξ_i are the natural coordinates. Similarly, the motion is described in terms of the current position \mathbf{x}_a of the *same* particles:

$$\mathbf{x} = \sum_{a=1}^n N_a \mathbf{x}_a. \quad (3.10)$$

Quantities such as displacement, velocity and virtual velocity can be discretized in a similar way.

In deriving the discretized equilibrium equations, the integrations performed over the entire volume can be written as a sum of integrations constrained to the volume of an element. For this reason, the discretized equations are defined in terms of integrations

over a particular element e . The discretized equilibrium equations for this particular element per node is given by

$$\delta W^e \phi, N_a \delta \mathbf{v} = \delta \mathbf{v}_a \cdot \mathbf{T}_a^e - \mathbf{F}_a^e, \quad (3.11)$$

where

$$\begin{aligned} T_a^e &= \int_{v^e} \sigma \nabla N_a dv, \text{ and} \\ F_a^e &= \int_{v^e} N_a \mathbf{f} dv + \int_{\partial v^e} N_a \mathbf{t} da. \end{aligned} \quad (3.12)$$

The linearization of the internal virtual work can be split into a *material* and an *initial stress* component [1]:

$$\begin{aligned} D\delta W_{\text{int}}^e \phi, \delta \mathbf{v} \mathbf{u} &= \int_{v^e} \delta \mathbf{d} : \mathbf{C} : \varepsilon dv + \int_{v^e} \boldsymbol{\sigma} : \left[\nabla \mathbf{u}^T \nabla \delta \mathbf{v} \right] dv \\ &= D\delta W_c^e \phi, \delta \mathbf{v} \mathbf{u} + D\delta W_\sigma^e \phi, \delta \mathbf{v} \mathbf{u}. \end{aligned} \quad (3.13)$$

The constitutive component can be discretized as follows:

$$D\delta W_c^e \phi, \delta \mathbf{v} \mathbf{u} = \delta \mathbf{v}_a \cdot \left(\int_{v^e} \mathbf{B}_a^T \mathbf{D} \mathbf{B}_b dv \right) \mathbf{u}_b. \quad (3.14)$$

The term in parentheses defines the constitutive component of the tangent matrix relating node a to node b in element e :

$$\mathbf{K}_{c,ab}^e = \int_{v^e} \mathbf{B}_a^T \mathbf{D} \mathbf{B}_b dv. \quad (3.15)$$

Here, the linear strain-displacement matrix \mathbf{B} relates the displacements to the small-strain tensor in Voigt Notation:

$$\underline{\boldsymbol{\varepsilon}} = \sum_{a=1}^n \mathbf{B}_a \mathbf{u}_a. \quad (3.16)$$

Or, written out completely,

$$\mathbf{B}_a = \begin{bmatrix} \partial N_a / \partial x & 0 & 0 \\ 0 & \partial N_a / \partial y & 0 \\ 0 & 0 & \partial N_a / \partial z \\ \partial N_a / \partial y & \partial N_a / \partial x & 0 \\ 0 & \partial N_a / \partial z & \partial N_a / \partial y \\ \partial N_a / \partial z & 0 & \partial N_a / \partial z \end{bmatrix}. \quad (3.17)$$

The spatial constitutive matrix \mathbf{D} is constructed from the components of the fourth-order tensor \mathbf{C} using the following table; $\mathbf{D}_{IJ} = \mathbf{C}_{ijkl}$ where

I/J	i/k	j/l
1	1	1
2	2	2
3	3	3

4	1	2
5	2	3
6	1	3

The initial stress component can be written as follows:

$$D\delta W_\sigma^e \phi, N_a \delta \mathbf{v} N_b \mathbf{u}_b = \int_{v^e} \nabla N_a \cdot \boldsymbol{\sigma} \nabla N_b \mathbf{I} dv. \quad (3.18)$$

For the pressure component of the external virtual work, we find

$$D\delta W_p^e \phi, N_a \delta \mathbf{v}_a N_b \mathbf{u}_b = \delta \mathbf{v}_a \cdot \mathbf{K}_{p,ab}^e \mathbf{u}_b, \quad (3.19)$$

where,

$$\begin{aligned} \mathbf{K}_{p,ab}^e &= \boldsymbol{\varepsilon} \mathbf{k}_{p,ab}^e, \quad \mathbf{k}_{p,ab}^e = \frac{1}{2} \int_{A_\xi} p \frac{\partial \mathbf{x}}{\partial \xi} \left(\frac{\partial N_a}{\partial \eta} N_b - \frac{\partial N_b}{\partial \eta} N_a \right) d\xi d\eta. \\ &+ \frac{1}{2} \int_{A_\eta} p \frac{\partial \mathbf{x}}{\partial \eta} \left(\frac{\partial N_a}{\partial \xi} N_b - \frac{\partial N_b}{\partial \xi} N_a \right) d\xi d\eta \end{aligned} \quad (3.20)$$

3.2. Newton-Raphson method

The Newton-Raphson method (also known as “Newton’s method”, “Full Newton method” or “the Newton method”) is the basis for solving the nonlinear finite element equations. This section will describe the *Full Newton method* and the Broyden-Fletcher-Goldfarb-Shanno (BFGS) method [7]. The latter variation is actually a *quasi-Newton method*. It is important since it provides several advantages over the full Newton method and it is this method that is implemented in FEBio [7].

3.2.1. Full Newton Method

The Newton-Raphson equation (3.3) can be written in terms of the discretized equilibrium equations that were derived in the previous section as follows:

$$\delta \mathbf{v}^T \cdot \mathbf{K} \cdot \mathbf{u} = -\delta \mathbf{v}^T \cdot \mathbf{R}. \quad (3.21)$$

Since the virtual velocities $\delta \mathbf{v}$ are arbitrary, a discretized Newton-Raphson scheme can be formulated as follows:

$$\mathbf{K} \mathbf{x}_k \cdot \mathbf{u} = -\mathbf{R} \mathbf{x}_k; \quad \mathbf{x}_{k+1} = \mathbf{x}_k + \mathbf{u}. \quad (3.22)$$

This is the basis of the Newton-Raphson method. For each iteration k , both the stiffness matrix and the residual vector are re-evaluated and a displacement increment \mathbf{u} is calculated by pre-multiplying both sides of the above equation by \mathbf{K}^{-1} . This procedure is repeated until some convergence criteria are satisfied.

The formation of the stiffness matrix and, especially, calculation of its inverse, are computationally expensive. Quasi-Newton methods do not require the reevaluation of the stiffness matrix for every iteration. Instead, a quick update is calculated. One particular method that has been quite successful in the field of computational solid mechanics is the BFGS method, which is described in the next section.

3.2.2. BFGS Method

The BFGS method updates the stiffness matrix (or rather its inverse) to provide an approximation to the exact matrix. A displacement increment is defined as

$$\mathbf{d}_k = \mathbf{x}_k - \mathbf{x}_{k-1}, \quad (3.23)$$

and an increment in the residual is defined as

$$\mathbf{G}_k = \mathbf{R}_{k-1} - \mathbf{R}_k. \quad (3.24)$$

The updated matrix \mathbf{K}_k should satisfy the quasi-Newton equation:

$$\mathbf{K}_k \mathbf{d}_k = \mathbf{G}_k. \quad (3.25)$$

In order to calculate this update, as displacement increment is first calculated:

$$\mathbf{u} = \mathbf{K}_{k-1}^{-1} \mathbf{R}_{k-1}. \quad (3.26)$$

This displacement vector defines a “direction” for the actual displacement increment. A line search (see next section) can now be applied to determine the optimal displacement increment:

$$\mathbf{x}_k = \mathbf{x}_{k-1} + s\mathbf{u}, \quad (3.27)$$

where s is determined from the line search. With the updated position calculated, \mathbf{R}_k can be evaluated. Also, using equations (3.23) and (3.24), \mathbf{d}_k and \mathbf{G}_k can be evaluated. The stiffness update can now be expressed as

$$\mathbf{K}_k^{-1} = \mathbf{A}_k^T \mathbf{K}_{k-1}^{-1} \mathbf{A}_k, \quad (3.28)$$

where the matrix \mathbf{A} is an $n \times n$ matrix of the simple form:

$$\mathbf{A}_k = \mathbf{I} + \mathbf{v}_k \mathbf{w}_k^T. \quad (3.29)$$

The vectors \mathbf{v} and \mathbf{w} are given by

$$\mathbf{v}_k = - \left(\frac{\mathbf{d}_k^T \mathbf{G}_k}{\mathbf{d}_k^T \mathbf{K}_{k-1} \mathbf{d}_k} \right)^{1/2} \mathbf{K}_{k-1} \mathbf{d}_k - \mathbf{G}_k, \quad (3.30)$$

$$\mathbf{w}_k = \frac{\mathbf{d}_k}{\mathbf{d}_k^T \mathbf{G}_k}. \quad (3.31)$$

The vector $\mathbf{K}_{k-1} \mathbf{d}_k$ is equal to $s\mathbf{R}_{k-1}$ and has already been calculated.

To avoid numerically dangerous updates, the condition number c of the updating matrix \mathbf{A} is calculated:

$$c = \left(\frac{\mathbf{d}_k^T \mathbf{G}_k}{\mathbf{d}_k^T \mathbf{K}_{k-1} \mathbf{d}_k} \right)^{1/2}. \quad (3.32)$$

The update is not performed when this number exceeds a preset tolerance.

Considering the actual computations involved, it should be noted that using the matrix updates defined above, the calculation of the search direction in (3.26) can be rewritten as,

$$\mathbf{u} = \mathbf{I} + \mathbf{w}_{k-1} \mathbf{v}_{k-1}^T \cdots \mathbf{I} + \mathbf{w}_1 \mathbf{v}_1^T \mathbf{K}_0^{-1} \mathbf{I} + \mathbf{v}_1 \mathbf{w}_1^T \cdots \mathbf{I} + \mathbf{v}_{k-1} \mathbf{w}_{k-1}^T \mathbf{R}_{k-1}. \quad (3.33)$$

Hence, the search direction can be computed without explicitly calculating the updated matrices or performing any additional costly matrix factorizations as required in the full Newton-Raphson method.

3.2.3. Line Search Method

A powerful technique often used to improve the convergence rate of Newton based methods is the *line search method*. In this method, the direction of the displacement vector \mathbf{u} is considered as optimal, but the magnitude is controlled by a parameter s :

$$\mathbf{x}_{k+1} = \mathbf{x}_k + s\mathbf{u}. \quad (3.34)$$

The value of s is usually chosen so that the total potential energy $W(s) = W(\mathbf{x}_k + s\mathbf{u})$ at the end of the iteration is minimized in the direction of \mathbf{u} . This is equivalent to the requirement that the residual force $\mathbf{R}(\mathbf{x}_k + s\mathbf{u})$ at the end of the iteration is orthogonal to \mathbf{u} :

$$\mathbf{R}(s) = \mathbf{u}^T \mathbf{R}(\mathbf{x}_k + s\mathbf{u}) = 0. \quad (3.35)$$

However, in practice it is sufficient to obtain a value of s such that,

$$|\mathbf{R}(s)| < \rho |\mathbf{R}(0)|, \quad (3.36)$$

where typically a value of $\rho = 0.9$ is used. Under normal conditions the value $s = 1$ automatically satisfies equation (3.36) and therefore few extra operations are involved. However, when this is not the case, a more suitable value for s needs to be obtained. For this reason it is convenient to approximate $\mathbf{R}(s)$ as a quadratic in s :

$$\mathbf{R}(s) \approx \mathbf{R}(0) + \mathbf{R}'(0)s + \frac{1}{2}\mathbf{R}''(0)s^2 = 0, \quad (3.37)$$

which yields a value for s as

$$s = \frac{r}{2} \pm \sqrt{\left(\frac{r}{2}\right)^2 - r}, \quad r = \frac{\mathbf{R}'(0)}{\mathbf{R}''(0)}. \quad (3.38)$$

If $r < 0$, the square root is positive and a first improved value for s is obtained:

$$s_1 = \frac{r}{2} + \sqrt{\left(\frac{r}{2}\right)^2 - r}. \quad (3.39)$$

If $r > 0$ the s can be obtained by using the value that minimizes the quadratic function, that is, $s_1 = r/2$. This procedure is now repeated with $\mathbf{R}'(0)$ replaced by $\mathbf{R}'(s_1)$ until equation (3.36) is satisfied.

Chapter 4. Element Library

FEBio provides several element types for finite element discretization. This chapter describes these elements in more detail.

4.1. Solid Elements

The 3D solid elements available in FEBio are *isoparametric elements*. All of the solid elements are formulated in a global Cartesian coordinate system. For all these elements, a local coordinate system (so-called *isoparametric coordinates*) is defined as well. The global position vector \mathbf{x} can be written as a function of the isoparametric coordinates in the following sense:

$$\mathbf{x}_{r,s,t} = \sum_{i=1}^n N_i(r,s,t) \mathbf{x}_i. \quad (4.1)$$

Here, n is the number of nodes, r , s and t are the isoparametric coordinates, N_i are the element shape functions and \mathbf{x}_i are the spatial coordinates of the element nodes. The same parametric interpolation is used for the interpolation of other scalar and vector quantities.

All elements in FEBio are integrated numerically. This implies that integrals over the volume of the element v^e are approximated by a sum:

$$\begin{aligned} \int_{v^e} f(\mathbf{x}) dv &= \int_{\square^e} f(\mathbf{r}) J(\mathbf{r}) d\square \\ &\cong \sum_{i=1}^m f(\mathbf{r}_i) J_i w_i. \end{aligned} \quad (4.2)$$

Here, \square is the biunit cube, m is the number of integration points, \mathbf{r}_i are the location of the integration points in isoparametric coordinates, J is the Jacobian of the transformation $\mathbf{x} = \mathbf{x}(r,s,t)$, and w_i is a weight associated with the integration point. The integration is performed over the element's volume in the natural coordinate system.

Most fully integrated solid elements are unsuitable for the analysis of (nearly-) incompressible material behavior. To deal with this type of deformation, a three-field element implementation is available in FEBio [8].

4.1.1. Hexahedral elements

FEBio implements an 8-node trilinear hexahedral element. This element is also known as a *brick* element. The shape functions for these elements are defined in function of the isoparametric coordinates r , s and t , and are given below.

$$\begin{aligned}
N_1 &= \frac{1}{2} \begin{bmatrix} 1-r & 1-s & 1-t \end{bmatrix} \\
N_2 &= \frac{1}{2} \begin{bmatrix} 1+r & 1-s & 1-t \end{bmatrix} \\
N_3 &= \frac{1}{2} \begin{bmatrix} 1+r & 1+s & 1-t \end{bmatrix} \\
N_4 &= \frac{1}{2} \begin{bmatrix} 1-r & 1+s & 1-t \end{bmatrix} \\
N_5 &= \frac{1}{2} \begin{bmatrix} 1-r & 1-s & 1+t \end{bmatrix} \\
N_6 &= \frac{1}{2} \begin{bmatrix} 1+r & 1-s & 1+t \end{bmatrix} \\
N_7 &= \frac{1}{2} \begin{bmatrix} 1+r & 1+s & 1+t \end{bmatrix} \\
N_8 &= \frac{1}{2} \begin{bmatrix} 1-r & 1+s & 1+t \end{bmatrix}
\end{aligned} \tag{4.3}$$

4.1.2. Pentahedral Elements

Pentahedral elements (also known as “wedge” elements) consist of six nodes and five faces. Their shape functions are defined in function of the isoparametric coordinates r , s and t and are given as follows.

$$\begin{aligned}
N_1 &= \frac{1}{2} \begin{bmatrix} 1-r-s & 1-t \end{bmatrix} \\
N_2 &= \frac{1}{2} r \begin{bmatrix} 1-t \end{bmatrix} \\
N_3 &= \frac{1}{2} s \begin{bmatrix} 1-t \end{bmatrix} \\
N_4 &= \frac{1}{2} \begin{bmatrix} 1-r-s & 1+t \end{bmatrix} \\
N_5 &= \frac{1}{2} r \begin{bmatrix} 1+t \end{bmatrix} \\
N_6 &= \frac{1}{2} s \begin{bmatrix} 1+t \end{bmatrix}
\end{aligned} \tag{4.4}$$

4.1.3. Tetrahedral Elements

Linear 4-node tetrahedral elements are also available in FEBio. Their shape functions are defined in function of the isoparametric coordinates r , s and t .

$$\begin{aligned}
 N_1 &= 1 - r - s - t \\
 N_2 &= r \\
 N_3 &= s \\
 N_4 &= t
 \end{aligned}
 \tag{4.5}$$

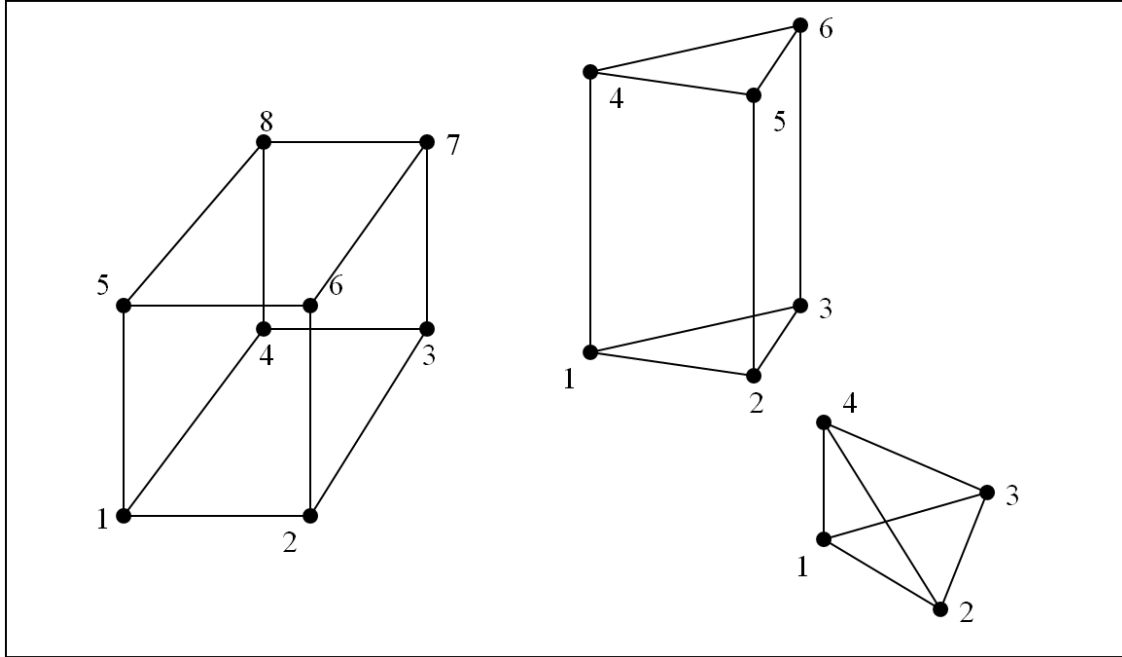


Figure 4-1. Different solid element types that are available in FEBio.

4.2. Shell Elements

Historically, shells have been formulated using two different approaches [9]. The difference between these approaches lies in the way the rotational degrees of freedom are defined. In the first approach, the rotational degrees of freedom are defined as angles. In addition, the plane stress condition needs to be enforced to take thickness variations into account. This approach is very useful for infinitesimal strains, but becomes very difficult to pursue in finite deformation due to the fact that finite rotations do not commute. Another disadvantage of this approach is that it requires a modification to the material formulation to enforce the plane stress condition. For complex materials this modification is very difficult or even impossible to obtain.

The alternative approach is to use an *extensible director* to describe the rotational degrees of freedom. With this approach it is not necessary to enforce the plane-stress condition and the full 3D constitutive relations can be employed. This approach is used in FEBio. A disadvantage of this approach is that it becomes difficult to enforce the unit length of the director throughout the entire element.

The shell formulation implemented in FEBio is still a work in progress. The goal is to implement an extensible director formulation with strain enhancements to deal with the

well-known locking effect in incompressible and bending problems [10]. With the current state of the implementation, it is advised to use a fine mesh in such problems.

4.2.1. Shell formulation

In FEBio an extensible director formulation is implemented [10]. Six degrees of freedom are assigned to each shell node: three displacement degrees of freedom and three director degrees of freedom. The position of any point in the shell can be written as:

$$\begin{aligned}
 \mathbf{X} \xi_i &= \bar{\mathbf{X}} \xi_\alpha + \mathbf{D} \xi_i, \\
 \bar{\mathbf{X}} \xi_\alpha &= \sum_{a=1}^n N_a \xi_\alpha \bar{\mathbf{X}}_a, \\
 \mathbf{D} \xi_i &= \sum_{a=1}^n N_a \xi_\alpha z_a \xi_3 \mathbf{D}_a, \\
 z_a \xi_3 &= \frac{1}{2} (1 + \xi_3 \left(\frac{h_a^0}{2} \right) - \frac{1}{2} (1 - \xi_3 \left(\frac{h_a^0}{2} \right)).
 \end{aligned} \tag{4.6}$$

It is assumed that Latin indices range from 1 to 3 and that Greek indices range from 1 to 2. The vector \mathbf{D} is called the *director* and it is assumed that $\|\mathbf{D}_a\| = 1$. (Note that this does not necessarily imply that $\|\mathbf{D}\| = 1$ throughout the entire shell.) The function z_a is the *thickness function* and evaluates the initial thickness of the shell, which at node a is given by h_a^0 .

Similarly, the displacement is given by

$$\begin{aligned}
 \mathbf{u} \xi_i &= \bar{\mathbf{u}} \xi_\alpha + \mathbf{t} \xi_i, \\
 \bar{\mathbf{u}} \xi_\alpha &= \sum_{a=1}^n N_a \xi_\alpha \bar{\mathbf{u}}_a, \\
 \mathbf{t} \xi_i &= \sum_{a=1}^n N_a \xi_\alpha z_a \xi_3 \mathbf{t}_a.
 \end{aligned} \tag{4.7}$$

The current configuration is then determined by

$$\begin{aligned}
 \mathbf{x} \xi_i &= \bar{\mathbf{x}} \xi_\alpha + \mathbf{d} \xi_i, \\
 \bar{\mathbf{x}} \xi_\alpha &= \bar{\mathbf{X}} \xi_\alpha + \bar{\mathbf{U}} \xi_\alpha, \\
 \mathbf{d} \xi_i &= \mathbf{D} \xi_i + \mathbf{t} \xi_i, \\
 \bar{\mathbf{x}}_a &= \bar{\mathbf{X}}_a + \bar{\mathbf{u}}_a, \\
 \mathbf{d}_a &= \mathbf{D}_a + \mathbf{t}_a.
 \end{aligned} \tag{4.8}$$

To take thickness variations into account, it is not required that \mathbf{d}_a is of unit length.

It is assumed that the virtual displacements have a similar interpolation than the actual displacements:

$$\delta \mathbf{u}_{\xi_i} = \sum_{a=1}^n N_a \xi_{\alpha} \delta \bar{\mathbf{u}}_a + \sum_{a=1}^n N_a \xi_{\alpha} z_a \xi_3 \delta \mathbf{t}_a. \quad (4.9)$$

The gradient of \mathbf{u} is given by

$$\nabla \mathbf{u} = \sum_{a=1}^n \nabla N_a \bar{\mathbf{u}}_a + \sum_{a=1}^n \nabla M_a \mathbf{t}_a. \quad (4.10)$$

where we have defined $M_a \xi_i = N_a \xi_{\alpha} z_a \xi_3$. And similarly for the gradient of the virtual displacement,

$$\nabla \delta \mathbf{u} = \sum_{a=1}^n \nabla N_a \delta \bar{\mathbf{u}}_a + \sum_{a=1}^n \nabla M_a \delta \mathbf{t}_a. \quad (4.11)$$

The internal virtual work is now given by

$$\begin{aligned} G_{\text{int}}^e &= \int_{\Omega^e} \boldsymbol{\sigma} : \nabla \delta \mathbf{u} dv \\ &= \sum_{a=1}^n \delta \bar{\mathbf{u}}_a \cdot \int_{\Omega^e} \boldsymbol{\sigma} \cdot \nabla N_a dv + \sum_{a=1}^n \delta \mathbf{t}_a \cdot \int_{\Omega^e} \boldsymbol{\sigma} \cdot \nabla M_a dv. \end{aligned} \quad (4.12)$$

The shell geometry suggests an integration of the following type:

$$\int_{\Omega^e} \boldsymbol{\sigma} \cdot dv = \int_{\square} \left(\int_{-1}^{+1} \boldsymbol{\sigma} \cdot j d\xi_3 \right) d\xi_1 d\xi_2. \quad (4.13)$$

where $j = \det \frac{\partial \mathbf{x}}{\partial \boldsymbol{\xi}}$ is the Jacobian of the transformation. In FEBio a 3-point Gaussian quadrature rule is used for the through-the-thickness integration.

FEBio currently supports four node quadrilateral and three-node triangular shell elements.

4.2.2. Quadrilateral shells

For quadrilateral shells, the shape functions are given by

$$\begin{aligned}
 N_1 &= \frac{1}{4} \begin{bmatrix} 1-r & 1-s \end{bmatrix} \\
 N_2 &= \frac{1}{4} \begin{bmatrix} 1+r & 1-s \end{bmatrix} \\
 N_3 &= \frac{1}{4} \begin{bmatrix} 1+r & 1+s \end{bmatrix} \\
 N_4 &= \frac{1}{4} \begin{bmatrix} 1-r & 1+s \end{bmatrix}
 \end{aligned}
 \tag{4.14}$$

4.2.3. Triangular shells

For triangular shell elements, the shape functions are given by

$$\begin{aligned}
 N_1 &= 1-r-s \\
 N_2 &= r \\
 N_3 &= s
 \end{aligned}
 \tag{4.15}$$

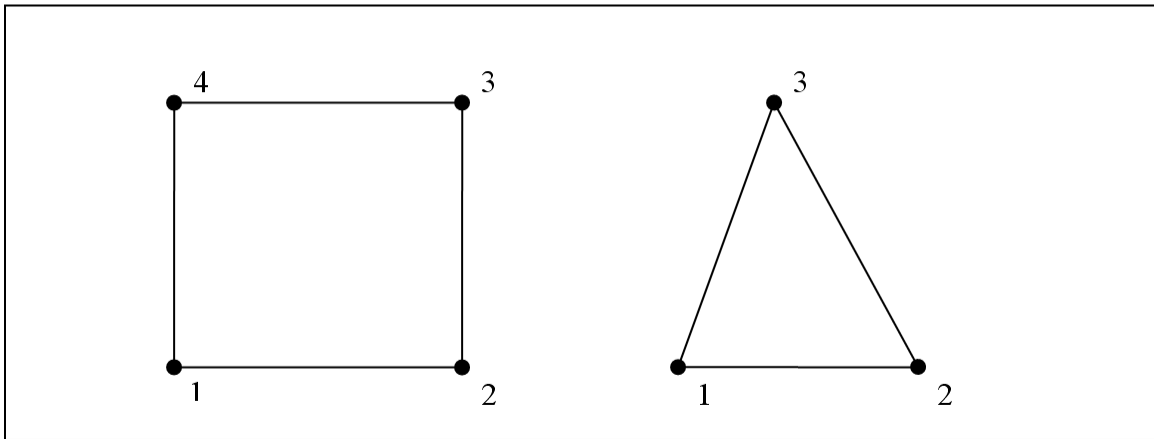


Figure 4-2. Different shell elements available in FEBio

Chapter 5. Constitutive Models

This chapter describes the theoretical background behind the constitutive models that are available in FEBio. Most materials are derived from a hyperelastic strain-energy function. Please consult section 2.4 for more background information on this type of material.

5.1. Linear Elasticity

In the theory of linear elasticity the Cauchy stress tensor is a linear function of the small strain tensor $\boldsymbol{\varepsilon}$:

$$\boldsymbol{\sigma} = \boldsymbol{\mathcal{C}} : \boldsymbol{\varepsilon}. \quad (5.1)$$

Here, $\boldsymbol{\mathcal{C}}$ is the fourth-order elasticity tensor that contains the material properties. In the most general case this tensor has 21 independent parameters. However, in the presence of material symmetry the number of independent parameters is greatly reduced. For example, in the case of isotropic linear elasticity only two independent parameters remain. In this case, the elasticity tensor is given by

$$\mathcal{C}_{ijkl} = \lambda \delta_{ij} \delta_{kl} + \mu (\delta_{ik} \delta_{jl} + \delta_{il} \delta_{jk}). \quad (5.2)$$

The material coefficients λ and μ are known as the Lamé parameters. Using this equation, the stress-strain relationship can be written as

$$\sigma_{ij} = \lambda \text{tr} \boldsymbol{\varepsilon} \delta_{ij} + 2\mu \varepsilon_{ij}. \quad (5.3)$$

If the stress and strain are represented as Voigt vectors, the constitutive equation can be rewritten in matrix form as

$$\begin{pmatrix} \sigma_{11} \\ \sigma_{22} \\ \sigma_{33} \\ \sigma_{12} \\ \sigma_{23} \\ \sigma_{13} \end{pmatrix} = \begin{pmatrix} \lambda + 2\mu & \lambda & \lambda & 0 & 0 & 0 \\ \lambda & \lambda + 2\mu & \lambda & 0 & 0 & 0 \\ \lambda & \lambda & \lambda + 2\mu & 0 & 0 & 0 \\ 0 & 0 & 0 & \mu & 0 & 0 \\ 0 & 0 & 0 & 0 & \mu & 0 \\ 0 & 0 & 0 & 0 & 0 & \mu \end{pmatrix} \begin{pmatrix} \varepsilon_{11} \\ \varepsilon_{22} \\ \varepsilon_{33} \\ \lambda_{12} \\ \lambda_{23} \\ \lambda_{13} \end{pmatrix}. \quad (5.4)$$

The strain measures λ_{ij} are the *engineering strains* and are given by $\lambda_{ij} = 2\varepsilon_{ij}$.

The following table relates the Lamé parameters to the more familiar Young's modulus E and Poisson's ratio ν or to the bulk modulus K and shear modulus G .

	E, ν	λ, μ	K, G
E, ν		$E = \frac{\mu}{\lambda + \mu} 2\mu + 3\lambda$ $\nu = \frac{\lambda}{2 \lambda + \mu}$	$E = \frac{9KG}{3K + G}$ $\nu = \frac{3K - 2G}{6K + 2G}$
λ, μ	$\lambda = \frac{\nu E}{1 + \nu} \frac{1 - 2\nu}{1 - 2\nu}$ $\mu = \frac{E}{2} \frac{1}{1 + \nu}$		$\lambda = K - \frac{2}{3}G$ $\mu = G$
K, G	$K = \frac{E}{3} \frac{1}{1 - 2\nu}$ $G = \frac{E}{2} \frac{1}{1 + \nu}$	$K = \lambda + \frac{2}{3}\mu$ $G = \mu$	

It is of some interest to note that the theoretical range of the Poisson's ratio for an isotropic material is $-1 \leq \nu \leq 0.5$. Materials with Poisson's ratio (close to) 0.5 are known as (nearly-) incompressible materials. For these materials, the bulk modulus approaches infinity. Most materials have a positive Poisson's ratio, although there do exist some materials with a negative ratio. These materials are known as *auxetic* materials and they have the remarkable property that they expand under tension.

The linear stress-strain relationship can also be derived from a strain-energy function such as in the case of hyperelastic materials. In this case the linear strain-energy is given by

$$W = \frac{1}{2} \boldsymbol{\varepsilon} : \mathbf{C} \boldsymbol{\varepsilon} . \quad (5.5)$$

The stress is then similarly derived from $\boldsymbol{\sigma} = \frac{\partial W}{\partial \boldsymbol{\varepsilon}}$. In the case of isotropic elasticity, (5.5) can be simplified:

$$W = \frac{1}{2} \lambda \text{tr} \boldsymbol{\varepsilon}^2 + \mu \boldsymbol{\varepsilon} : \boldsymbol{\varepsilon} . \quad (5.6)$$

The Cauchy stress is now given by

$$\boldsymbol{\sigma} = \lambda \text{tr} \boldsymbol{\varepsilon} \mathbf{1} + 2\mu \boldsymbol{\varepsilon} . \quad (5.7)$$

5.2. Isotropic Elasticity

The linear elastic material model as described in section 5.1 is only valid for small strains and small rotations. A first modification to this model to the range of nonlinear deformations is given by the St. Venant-Kirchhoff model [1], which in FEBio is referred to as *isotropic elasticity*. This model is objective for large strains and rotations. For the isotropic case it can be derived from the following hyperelastic strain-energy function:

$$W = \frac{1}{2} \lambda \text{tr} \mathbf{E}^2 + \mu \mathbf{E} : \mathbf{E}. \quad (5.8)$$

The second Piola-Kirchhoff stress can be derived from this:

$$\mathbf{S} = \frac{\partial W}{\partial \mathbf{E}} = \lambda \text{tr} \mathbf{E} \mathbf{1} + 2\mu \mathbf{E}. \quad (5.9)$$

Note that these equations are similar to the corresponding equations in the linear elastic case, only the small strain tensor is replaced by the Lagrangian elasticity tensor \mathbf{E} .

5.3. Neo-Hookean Hyperelasticity

This is a compressible neo-Hookean material. It is derived from the following hyperelastic strain energy function [1]:

$$W = \frac{\mu}{2} (I_1 - 3) - \mu \ln J + \frac{\lambda}{2} (\ln J)^2.$$

The parameters μ and λ are the Lamé parameters from linear elasticity. This model reduces to the isotropic linear elastic model for small strains and rotations.

The neo-Hookean material is an extension of Hooke's law for the case of large deformations. It is useable for plastics and rubber-like substances. A generalization of this model is the Mooney-Rivlin material, which is often used to describe the elastic response of biological tissue.

In FEBio this constitutive model uses a standard displacement-based element formulation and a "coupled" strain energy, so care must be taken when modeling materials with nearly-incompressible material behavior to avoid element locking.

5.4. Mooney-Rivlin Hyperelasticity

This material model is a hyperelastic Mooney-Rivlin type with uncoupled deviatoric and volumetric behavior. The uncoupled strain energy W is given by:

$$W = C_1 (\tilde{I}_1 - 3) + C_2 (\tilde{I}_2 - 3) + \frac{1}{2} K (\ln J)^2.$$

C_1 and C_2 are the Mooney-Rivlin material coefficients, \tilde{I}_1 and \tilde{I}_2 are the invariants of the deviatoric part of the right Cauchy-Green deformation tensor, $\tilde{\mathbf{C}} = \tilde{\mathbf{F}}^T \tilde{\mathbf{F}}$, where $\tilde{\mathbf{F}} = J^{(-1/3)} \mathbf{F}$, \mathbf{F} is the deformation gradient and $J = \det \mathbf{F}$ is the Jacobian of the deformation. When $C_2 = 0$, this model reduces to an uncoupled version of the

incompressible neo-Hookean constitutive model. This material model uses a three-field element formulation, interpolating displacements as linear field variables and pressure and volume ratio as piecewise constant in each element [8].

5.5. Ogden Hyperelastic

The Ogden material is defined using the following hyperelastic strain energy function:

$$W(\lambda_1, \lambda_2, \lambda_3, J) = \sum_{i=1}^N \frac{c_i}{m_i^2} \tilde{\lambda}_1^{m_i} + \tilde{\lambda}_2^{m_i} + \tilde{\lambda}_3^{m_i} - 3 + U(J) \quad (5.10)$$

Here, $\tilde{\lambda}_i$ are the deviatoric principal stretches and c_i and m_i are material parameters. The term $U(J)$ is the volumetric component and J is the determinant of the deformation gradient.

Note that the neo-Hookean and Mooney-Rivlin models can also be obtained from the general Ogden strain energy function using special choices for c_i and m_i .

5.6. Veronda-Westmann Hyperelasticity

This model is similar to the Mooney-Rivlin model in that it also uses an uncoupled strain energy. However, in this case the strain energy is given by an exponential form:

$$W = C_1 \left[e^{C_2 \tilde{I}_1 - 3} - 1 \right] - \frac{C_1 C_2}{2} \tilde{I}_2 - 3 + U(J) \quad (5.11)$$

The dilatational term U is identical to the Mooney-Rivlin model.

This material model was the result from the research of the elastic response of skin tissue [11].

5.7. Transversely Isotropic Hyperelastic

This constitutive model can be used to represent a material that has a single preferred fiber direction and was developed for application to biological soft tissues [3, 12, 13]. It can be used to model tissues such as tendons, ligaments and muscle. The elastic response of the tissue is assumed to arise from the resistance of the fiber family and an isotropic matrix. It is assumed that the strain energy function can be written as follows:

$$W = F_1(\tilde{I}_1, \tilde{I}_2) + F_2(\tilde{\lambda}) + \frac{K}{2} [\ln J]^2 \quad (5.12)$$

Here \tilde{I}_1 and \tilde{I}_2 are the first and second invariants of the deviatoric version of the right Cauchy Green deformation tensor $\tilde{\mathbf{C}}$ and $\tilde{\lambda}$ is the deviatoric part of the stretch along the fiber direction ($\tilde{\lambda}^2 = \mathbf{a}_0 \cdot \tilde{\mathbf{C}} \cdot \mathbf{a}_0$, where \mathbf{a}_0 is the initial fiber direction), and $J = \det \mathbf{F}$ is the Jacobian of the deformation (volume ratio). The function F_1 represents the material response of the isotropic ground substance matrix, while F_2 represents the contribution from the fiber family. The strain energy of the fiber family is as follows:

$$\begin{aligned}
\tilde{\lambda} \frac{\partial F_2}{\partial \tilde{\lambda}} &= 0, \quad \tilde{\lambda} \leq 1; \\
\tilde{\lambda} \frac{\partial F_2}{\partial \tilde{\lambda}} &= C_3 e^{C_4 \tilde{\lambda} - 1}, \quad 1 < \tilde{\lambda} < \lambda_m; \\
\tilde{\lambda} \frac{\partial F_2}{\partial \tilde{\lambda}} &= C_5 + C_6 \tilde{\lambda}, \quad \tilde{\lambda} \geq \lambda_m.
\end{aligned} \tag{5.13}$$

Here, λ_m is the stretch at which the fibers are straightened, C_3 scales the exponential stresses, C_4 is the rate of uncrimping of the fibers, and C_5 is the modulus of the straightened fibers. C_6 is determined from the requirement that the stress is continuous at λ_m .

This material model uses a three-field element formulation, interpolating displacements as linear field variables and pressure and volume ratio as piecewise constant on each element [8].

5.8. Biphasic Material

The biphasic material model differs significantly from the previous material models in that it also requires the explicit modeling of fluid that permeates the solid. The biphasic material model is useful to simulate materials that show viscoelastic behavior due to the presence of a fluid. Several biological materials such as cartilage can be described more accurately this way.

The finite element formulation for the biphasic material differs significantly from the standard solid displacement-only formulation in Chapter 3. This is a consequence of the need to introduce a new field variable, namely the fluid pressure p , which requires a coupled displacement-fluid pressure system to be solved. This section describes this formulation.

5.8.1. Governing Equations

Consider a mixture consisting of a solid constituent and a fluid constituent. Both constituents are considered to be intrinsically incompressible, but the mixture can change volume when fluid enters or leaves the porous solid matrix [14, 15]. According to the kinematics of the continuum [16], each constituent α of a mixture ($\alpha = s$ for the solid and $\alpha = w$ for the fluid) has a separate motion $\chi^\alpha: \mathbf{X}^\alpha, t \rightarrow \mathbf{x}$ which places particles of each mixture constituent, originally located at \mathbf{X}^α , in the current configuration \mathbf{x} according to

$$\mathbf{x} = \chi^\alpha(\mathbf{X}^\alpha, t). \quad (5.14)$$

For the purpose of finite element analyses, the motion of the solid matrix, $\alpha = s$, is of particular interest.

The governing equations that enter into the statement of virtual work are the conservation of linear momentum and the conservation of mass, for the mixture as a whole. Under quasi-static conditions, in the absence of external body forces, the conservation of momentum reduces to

$$\text{div } \mathbf{T} = \mathbf{0}, \quad (5.15)$$

where \mathbf{T} is the Cauchy stress for the mixture. Since the mixture is porous, this stress may also be written as

$$\mathbf{T} = -p\mathbf{I} + \mathbf{T}^e, \quad (5.16)$$

where p is the fluid pressure and \mathbf{T}^e is the effective or extra stress, resulting from the deformation of the solid matrix. Conservation of mass for the mixture requires that

$$\text{div } \mathbf{v}^s + \mathbf{w} = 0, \quad (5.17)$$

where $\mathbf{v}^s = \partial \chi^s / \partial t$ is the solid matrix velocity and \mathbf{w} is the flux of the fluid relative to the solid matrix. Let the solid matrix displacement be denoted by \mathbf{u} , then $\mathbf{v}^s = \dot{\mathbf{u}}$.

To relate the relative fluid flux \mathbf{w} to the fluid pressure and solid deformation, it is necessary to employ the equation of conservation of linear momentum for the fluid,

$$-\phi^w \text{grad } p + \hat{\mathbf{p}}_d^w = \mathbf{0} \quad (5.18)$$

where ϕ^w is the solid matrix porosity, and $\hat{\mathbf{p}}_d^w$ is the momentum exchange between the solid and fluid constituents, typically representing the frictional interaction between these

constituents. This equation neglects the viscous stress of the fluid in comparison to $\hat{\mathbf{p}}_d^w$. The most common constitutive relation is $\hat{\mathbf{p}}_d^w = -\varphi^w \mathbf{K}^{-1} \cdot \mathbf{w}$, where the second order, symmetric tensor \mathbf{K} is the hydraulic permeability of the mixture. When combined with Eq.(5.18), it produces

$$\mathbf{w} = -\mathbf{K} \cdot \text{grad } p, \quad (5.19)$$

which is equivalent to Darcy's law. In general, \mathbf{K} may be a function of the deformation.

5.8.2. Weak Formulation

A weak form of the statement conservation of linear momentum for the quasi-static case is obtained by using Eqs.(5.15) and (5.17):

$$\int_b \left[\delta \mathbf{v}^s \cdot \text{div } \mathbf{T} + \delta p \text{ div } \mathbf{v}^s + \mathbf{w} \right] dv = 0, \quad (5.20)$$

where b is the domain of interest defined on the solid matrix, $\delta \mathbf{v}^s$ is a virtual velocity of the solid, and δp is a virtual pressure of the fluid [17]; dv is an elemental volume of b . Using the divergence theorem, this expression may be rearranged as

$$\delta W = \int_b \mathbf{T} : \delta \mathbf{D}^s dv - \int_{\partial b} \delta \mathbf{v}^s \cdot \mathbf{t} da + \int_b \mathbf{w} \cdot \text{grad } \delta p - \delta p \text{ div } \mathbf{v}^s dv - \int_{\partial b} \delta p w_n da = 0, \quad (5.21)$$

where $\delta \mathbf{D}^s = \text{grad } \delta \mathbf{v}^s + \text{grad}^T \delta \mathbf{v}^s / 2$ is the virtual rate of deformation tensor, $\mathbf{t} = \mathbf{T} \cdot \mathbf{n}$ is the total traction on the surface ∂b , and $w_n = \mathbf{w} \cdot \mathbf{n}$ is the component of the fluid flux normal to ∂b , with \mathbf{n} representing the unit outward normal to ∂b ; da represents an elemental area of ∂b . In this type of problem, essential boundary conditions are prescribed on \mathbf{u} and p , and natural boundary conditions on \mathbf{t} and w_n . In the expression of Eq.(5.21), δW , χ^s , p , $\delta \mathbf{v}^s$, δp represents the virtual work.

Since the system of equations in Eq.(5.21) is highly nonlinear, its solution requires an iterative scheme such as Newton's method. This requires the linearization of δW at some trial solution χ_k^s, p_k , along an increment $\Delta \mathbf{u}$ in χ^s and an increment Δp in p ,

$$\delta W + D\delta W \Delta \mathbf{u} + D\delta W \Delta p = 0, \quad (5.22)$$

where $Df \Delta q$ represents the directional derivative of f along Δq . For convenience, the virtual work may be separated into its internal and external parts,

$$\delta W = \delta W_{\text{int}} - \delta W_{\text{ext}}, \quad (5.23)$$

where

$$\delta W_{\text{int}} = \int_b \mathbf{T} : \delta \mathbf{D}^s dv + \int_b \mathbf{w} \cdot \text{grad } \delta p - \delta p \text{ div } \mathbf{v}^s dv, \quad (5.24)$$

and

$$\delta W_{\text{ext}} = \int_{\partial b} \delta \mathbf{v}^s \cdot \mathbf{t} da + \int_{\partial b} \delta p w_n da. \quad (5.25)$$

The evaluation of the directional derivatives can be performed following a standard approach [1]. For the internal part of the virtual work, the directional derivative along $\Delta \mathbf{u}$ yields

$$\begin{aligned}
D\delta W_{\text{int}} \Delta \mathbf{u} = & \int_b \delta \mathbf{D}^s : \mathcal{C} : \Delta \boldsymbol{\varepsilon} dv + \int_b \mathbf{T} : \text{grad}^T \Delta \mathbf{u} \cdot \text{grad} \delta \mathbf{v}^s dv \\
& - \int_b \delta p \left(\left[\text{div} \Delta \mathbf{u} \mathbf{I} - \text{grad}^T \Delta \mathbf{u} \right] : \text{grad} \mathbf{v}^s + \text{div} \dot{\Delta \mathbf{u}} \right) dv, \quad (5.26) \\
& - \int_b \text{grad} \delta p \cdot \mathcal{K} : \Delta \boldsymbol{\varepsilon} \cdot \text{grad} p dv
\end{aligned}$$

where \mathcal{C} is the fourth-order spatial elasticity tensor for the mixture and $\Delta \boldsymbol{\varepsilon} = \text{grad} \Delta \mathbf{u} + \text{grad}^T \Delta \mathbf{u} / 2$. Based on the relation of Eq.(5.16), the spatial elasticity tensor may also be expanded as

$$\mathcal{C} = \mathcal{C}^e + p \mathbf{I} \otimes \mathbf{I} + 2\mathbf{I} \bar{\otimes} \mathbf{I}, \quad (5.27)$$

where \mathcal{C}^e is the spatial elasticity tensor for the solid matrix [18].¹ It is related to the material elasticity tensor \mathbb{C}^e via

$$\mathcal{C}^e = J^{-1} \mathbf{F} \otimes \mathbf{F} : \mathbb{C}^e : \mathbf{F}^T \otimes \mathbf{F}^T, \quad (5.28)$$

where $\mathbf{F} = \text{Grad} \boldsymbol{\chi}^s$ is the deformation gradient of the solid matrix. As usual in hyperelasticity, $\mathbb{C}^e = \partial \mathbf{S}^e / \partial \mathbf{E}$ where \mathbf{E} is the Lagrangian strain tensor and \mathbf{S}^e is the second Piola-Kirchhoff stress tensor, related to the Cauchy stress tensor via $\mathbf{T}^e = J^{-1} \mathbf{F} \cdot \mathbf{S}^e \cdot \mathbf{F}^T$. Since \mathbf{S}^e may be obtained from a strain energy density function Ψ according to $\mathbf{S}^e = \partial \Psi / \partial \mathbf{E}$, it follows that the material and spatial elasticity tensors exhibit two minor symmetries and one major symmetry.

Similarly, \mathcal{K} is a fourth-order tensor that represents the spatial measure of the rate of change of permeability with strain. It is related to its material frame equivalent \mathbb{K} via

$$\mathcal{K} = J^{-1} \mathbf{F} \otimes \mathbf{F} : \mathbb{K} : \mathbf{F}^T \otimes \mathbf{F}^T, \quad (5.29)$$

where $\mathbb{K} = \partial \mathbf{K}_0 / \partial \mathbf{E}$ and \mathbf{K}_0 is the permeability tensor in the material frame, such that $\mathbf{K} = J^{-1} \mathbf{F} \cdot \mathbf{K}_0 \cdot \mathbf{F}^T$. Since \mathbf{K}_0 and \mathbf{E} are symmetric tensors, it follows that \mathbb{K} and \mathcal{K} exhibit two minor symmetries (e.g., $\mathcal{K}_{jikl} = \mathcal{K}_{ijkl}$ and $\mathcal{K}_{ijlk} = \mathcal{K}_{ijkl}$); however, unlike the elasticity tensor, it is not necessary that these tensors exhibit major symmetry (e.g., $\mathcal{K}_{klj} \neq \mathcal{K}_{ijl}$ in general).

The directional derivative of δW_{int} along Δp is given by

$$D\delta W_{\text{int}} \Delta p = - \int_b \text{grad} \delta p \cdot \mathbf{K} \cdot \text{grad} \Delta p dv - \int_b \Delta p \text{div} \delta \mathbf{v}^s dv. \quad (5.30)$$

Note that letting $p=0$ and $\delta p=0$ in the above equations recovers the virtual work relations for nonlinear elasticity of compressible solids. The resulting simplified equation emerging from Eq.(5.26) is symmetric to interchanges of $\Delta \mathbf{u}$ and $\delta \mathbf{v}^s$, producing a symmetric stiffness matrix in the finite element formulation [1]. However, the general

¹ The dyadic products of second order tensors \mathbf{A} and \mathbf{B} are defined such that $\mathbf{A} \otimes \mathbf{B} : \mathbf{X} = \mathbf{B} : \mathbf{X} \mathbf{A}$, $\mathbf{A} \bar{\otimes} \mathbf{B} : \mathbf{X} = \mathbf{A} \cdot \mathbf{X} \cdot \mathbf{B}^T$, and $\mathbf{A} \bar{\otimes} \mathbf{B} : \mathbf{X} = \mathbf{A} \cdot \mathbf{X} \cdot \mathbf{B}^T + \mathbf{B} \cdot \mathbf{X}^T \cdot \mathbf{A}^T / 2$ for any second order tensor \mathbf{X} .

relations of Eqs.(5.26) and (5.30) do not exhibit symmetry to interchanges of $\Delta \mathbf{u}, \Delta p$ and $\delta \mathbf{v}^s, \delta p$, implying that the finite element stiffness matrix for a solid-fluid mixture is not symmetric under general conditions.

The directional derivatives of the external virtual work δW_{ext} depend on the type of boundary conditions being considered. For a prescribed total normal traction t_n , where $\mathbf{t} = t_n \mathbf{n}$,

$$\delta W_{\text{ext}}^t = \int_{\partial b} \delta \mathbf{v}^s \cdot t_n \mathbf{n} da \quad (5.31)$$

and

$$D\delta W_{\text{ext}}^t \Delta \mathbf{u} = \int_{\partial b} \delta \mathbf{v}^s \cdot t_n \left(\mathbf{g}_1 \times \frac{\partial \Delta \mathbf{u}}{\partial \eta^2} - \mathbf{g}_2 \times \frac{\partial \Delta \mathbf{u}}{\partial \eta^1} \right) \frac{da}{|\mathbf{g}_1 \times \mathbf{g}_2|} \quad (5.32)$$

$$D\delta W_{\text{ext}}^t \Delta p = 0$$

where

$$\mathbf{g}_\alpha = \frac{\partial \mathbf{x}}{\partial \eta^\alpha}, \quad \alpha = 1, 2 \quad (5.33)$$

are covariant basis (tangent) vectors on ∂b , such that

$$\mathbf{n} = \frac{\mathbf{g}_1 \times \mathbf{g}_2}{|\mathbf{g}_1 \times \mathbf{g}_2|} \quad (5.34)$$

For a prescribed normal effective traction t_n^e , where $\mathbf{t} = -p + t_n^e \mathbf{n}$ and p is not prescribed, then

$$\delta W_{\text{ext}}^e = \int_{\partial b} \delta \mathbf{v}^s \cdot (-p + t_n^e \mathbf{n}) da \quad (5.35)$$

and

$$D\delta W_{\text{ext}}^e \Delta \mathbf{u} = \int_{\partial b} \delta \mathbf{v}^s \cdot (-p + t_n^e \mathbf{n}) \left(\mathbf{g}_1 \times \frac{\partial \Delta \mathbf{u}}{\partial \eta^2} - \mathbf{g}_2 \times \frac{\partial \Delta \mathbf{u}}{\partial \eta^1} \right) \frac{da}{|\mathbf{g}_1 \times \mathbf{g}_2|} \quad (5.36)$$

$$D\delta W_{\text{ext}}^e \Delta p = - \int_{\partial b} \delta \mathbf{v}^s \cdot \Delta p \mathbf{n} da$$

Finally, for a prescribed normal fluid flux $w_n = \mathbf{w} \cdot \mathbf{n}$,

$$\delta W_{\text{ext}}^w = \int_{\partial b} \delta p w_n da \quad (5.37)$$

and

$$D\delta W_{\text{ext}}^w \Delta \mathbf{u} = \int_{\partial b} \delta p w_n \mathbf{n} \cdot \left(\mathbf{g}_1 \times \frac{\partial \Delta \mathbf{u}}{\partial \eta^2} - \mathbf{g}_2 \times \frac{\partial \Delta \mathbf{u}}{\partial \eta^1} \right) \frac{da}{|\mathbf{g}_1 \times \mathbf{g}_2|} \quad (5.38)$$

$$D\delta W_{\text{ext}}^w \Delta p = 0$$

5.8.3. Finite Element Equations

Let

$$\begin{aligned}\delta \mathbf{v}^s &= \sum_{a=1}^m N_a \delta \mathbf{v}_a & \delta p &= \sum_{a=1}^m N_a \delta p_a \\ \Delta \mathbf{u} &= \sum_{b=1}^m N_b \Delta \mathbf{u}_b & \Delta p &= \sum_{b=1}^m N_b \Delta p_b\end{aligned}\tag{5.39}$$

where N_a represents the interpolation functions over an element, $\delta \mathbf{v}_a, \delta p_a, \Delta \mathbf{u}_b, \Delta p_b$ respectively represent nodal values of $\delta \mathbf{v}^s, \delta p, \Delta \mathbf{u}, \Delta p$, and m is the number of nodes in an element. Then the discretized form of δW_{int} in Eq.(5.24) may be written as

$$\delta W_{\text{int}} = \sum_{e=1}^{n_e} \sum_{k=1}^{n_{\text{int}}^e} W_k J_\eta \sum_{a=1}^m \delta \mathbf{v}_a \quad \delta p_a \cdot \begin{bmatrix} \mathbf{r}_a^u \\ r_a^p \end{bmatrix}\tag{5.40}$$

where n_e is the number of elements in b , n_{int}^e is the number of integration points in the e -th element, W_k is the quadrature weight associated with the k -th integration point, and J_η is the Jacobian of the transformation from the spatial frame to the parametric space of the element. In the above expression,

$$\mathbf{r}_a^u = \mathbf{T} \cdot \nabla N_a \quad r_a^p = \mathbf{w} \cdot \nabla N_a - N_a \text{div} \mathbf{v}^s\tag{5.41}$$

and it is understood that J_η , \mathbf{r}_a^u and r_a^p are evaluated at the parametric coordinates of the k -th integration point.

Similarly, the discretized form of $D\delta W_{\text{int}}$ in Eq.(5.26) may be written as

$$-D\delta W_{\text{int}} = \sum_{e=1}^{n_e} \sum_{k=1}^{n_{\text{int}}^e} W_k J_\eta \sum_{a=1}^m \delta \mathbf{v}_a \quad \delta p_a \cdot \sum_{b=1}^m \begin{bmatrix} \mathbf{K}_{ab}^{uu} & \mathbf{k}_{ab}^{up} \\ \mathbf{k}_{ab}^{pu} & k_{ab}^{pp} \end{bmatrix} \cdot \begin{bmatrix} \Delta \mathbf{u}_b \\ \Delta p_b \end{bmatrix}\tag{5.42}$$

where

$$\begin{aligned}\mathbf{K}_{ab}^{uu} &= \nabla N_a \cdot \mathcal{C} \cdot \nabla N_b + \nabla N_a \cdot \mathbf{T} \cdot \nabla N_b \quad \mathbf{I} \\ \mathbf{k}_{ab}^{up} &= -N_b \nabla N_a \\ \mathbf{k}_{ab}^{pu} &= -\nabla N_a \cdot \mathcal{K} \cdot \nabla N_b \cdot \text{grad } p - N_a \left[\left(\text{div} \mathbf{v}^s + \frac{1}{\Delta t} \right) \mathbf{I} - \text{grad}^T \mathbf{v}^s \right] \cdot \nabla N_b \\ k_{ab}^{pp} &= -\nabla N_a \cdot \mathbf{K} \cdot \nabla N_b\end{aligned}\tag{5.43}$$

and Δt is a discrete increment in time. In a numerical implementation, it has been found that evaluating $\text{div} \mathbf{v}^s$ from \dot{J}/J , where $J = \det \mathbf{F}$, yields more accurate solutions than evaluating it from the trace of $\text{grad} \mathbf{v}^s$ [19].

For the various types of contributions to the external virtual work, a similar discretization produces

$$\delta W_{\text{ext}} = \sum_{e=1}^{n_e} \sum_{k=1}^{n_{\text{int}}^e} W_k J_\eta \sum_{a=1}^m \delta \mathbf{v}_a \quad \delta p_a \cdot \begin{bmatrix} \mathbf{r}_a^u \\ r_a^p \end{bmatrix}\tag{5.44}$$

and

$$-D\delta W_{\text{ext}} = \sum_{e=1}^{n_e} \sum_{k=1}^{n_{\text{int}}^e} W_k J_\eta \sum_{a=1}^m \delta \mathbf{v}_a \quad \delta p_a \cdot \sum_{b=1}^m \begin{bmatrix} \mathbf{K}_{ab}^{uu} & \mathbf{k}_{ab}^{up} \\ \mathbf{k}_{ab}^{pu} & k_{ab}^{pp} \end{bmatrix} \cdot \begin{bmatrix} \Delta \mathbf{u}_b \\ \Delta p_b \end{bmatrix}\tag{5.45}$$

where

$$J_\eta = |\mathbf{g}_1 \times \mathbf{g}_2| \quad (5.46)$$

In this case, m represents the number of nodes on an element face. For a prescribed normal traction t_n as given in (5.31)-(5.32),

$$\begin{aligned} \mathbf{r}_a^u &= t_n N_a \mathbf{n}, \quad r_a^u = 0 \\ \mathbf{K}_{ab}^{uu} &= t_n N_a \frac{1}{J_\eta} \mathcal{A} \left\{ \frac{\partial N_b}{\partial \eta^1} \mathbf{g}_2 - \frac{\partial N_b}{\partial \eta^2} \mathbf{g}_1 \right\}, \quad \mathbf{k}_{ab}^{up} = \mathbf{0} \\ \mathbf{k}_{ab}^{pu} &= \mathbf{0}, \quad k_{ab}^{pp} = 0 \end{aligned} \quad (5.47)$$

where $\mathcal{A} \mathbf{v} = -\mathcal{E} \cdot \mathbf{v}$ is the skew-symmetric tensor whose dual vector is \mathbf{v} and \mathcal{E} is the third-order permutation pseudo-tensor. For a prescribed traction t_n^e as given in (5.35)-(5.36),

$$\begin{aligned} \mathbf{r}_a^u &= -p + t_n^e N_a \mathbf{n}, \quad r_a^u = 0 \\ \mathbf{K}_{ab}^{uu} &= -p + t_n^e N_a \frac{1}{J_\eta} \mathcal{A} \left\{ \frac{\partial N_b}{\partial \eta^1} \mathbf{g}_2 - \frac{\partial N_b}{\partial \eta^2} \mathbf{g}_1 \right\}, \quad \mathbf{k}_{ab}^{up} = N_a N_b \mathbf{n} \\ \mathbf{k}_{ab}^{pu} &= \mathbf{0}, \quad k_{ab}^{pp} = 0 \end{aligned} \quad (5.48)$$

For a prescribed normal fluid flux w_n as given in (5.37)-(5.38),

$$\begin{aligned} \mathbf{r}_a^u &= \mathbf{0}, \quad r_a^u = w_n N_a \\ \mathbf{K}_{ab}^{uu} &= \mathbf{0}, \quad \mathbf{k}_{ab}^{up} = \mathbf{0} \\ \mathbf{k}_{ab}^{pu} &= w_n N_a \frac{1}{J_\eta} \mathbf{n} \times \left(\frac{\partial N_b}{\partial \eta^1} \mathbf{g}_2 - \frac{\partial N_b}{\partial \eta^2} \mathbf{g}_1 \right), \quad k_{ab}^{pp} = 0 \end{aligned} \quad (5.49)$$

5.9. Active Contraction Model

A time varying “elastance” active contraction model [20] was added to the transversely isotropic materials. When active contraction is activated, the total Cauchy stress $\boldsymbol{\sigma}$ is defined as the sum of the active stress tensor $\boldsymbol{\sigma}^a = T^a \mathbf{a} \otimes \mathbf{a}$ and the passive stress tensor $\boldsymbol{\sigma}^p$:

$$\boldsymbol{\sigma} = \boldsymbol{\sigma}^p + \boldsymbol{\sigma}^a, \quad (5.50)$$

where \mathbf{a} is the deformed fiber vector (unit length), defined as $\lambda \mathbf{a} = \mathbf{F} \cdot \mathbf{a}_0$. The time varying elastance model is a modification of the standard Hill equation that scales the standard equation by an activation curve $C(t)$. The active fiber stress T^a is defined as:

$$T^a = T_{\max} \frac{Ca_0^2}{Ca_0^2 + ECa_{50}^2} C(t), \quad (5.51)$$

where $T_{\max} = 135.7$ KPa is the isometric tension under maximal activation at the peak intracellular calcium concentration of $Ca_0 = 4.35$ μM . The length dependent calcium sensitivity is governed by the following equation:

$$ECa_{50} = \frac{(Ca_0)_{\max}}{\sqrt{\exp[B(l - l_0)] - 1}}, \quad (5.52)$$

where $(Ca_0)_{\max} = 4.35$ μM is the maximum peak intracellular calcium concentration, $B = 4.75$ μm^{-1} governs the shape of the peak isometric tension-sarcomere length relation, $l_0 = 1.58$ μm is the sarcomere length at which no active tension develops, and l is the sarcomere length which is the product of the fiber stretch λ and the sarcomere unloaded length $l_r = 2.04$ μm .

Chapter 6. Contact and Coupling

FEBio allows the user to connect the different parts of the model in various ways. Deformable parts can be connected to rigid bodies. Deformable objects can be brought in contact with each other. Rigid bodies can be connected with rigid joints. This chapter describes the different ways to couple parts together.

6.1. Rigid-Deformable Coupling

In FEBio deformable meshes can be coupled with rigid bodies. The coupling requires a modification of the global stiffness matrix. Additionally, degrees of freedom need to be introduced for the rigid bodies [21]. This section describes the coupling between rigid and deformable bodies.

6.1.1. Kinematics

The position vector \mathbf{x} of a finite element node may be denoted as,

$$\mathbf{x} = \mathbf{X} + \mathbf{u}, \quad (6.1)$$

where \mathbf{X} is the initial position of the node and \mathbf{u} the displacement vector. If this node is connected to a rigid body the position can alternatively be written as,

$$\mathbf{x} = \mathbf{r} + \mathbf{a}, \quad (6.2)$$

where \mathbf{r} is the current position of the center of mass of the rigid body and \mathbf{a} is the relative position of the node to the center of mass. The vector \mathbf{a} may be written in terms of its initial value \mathbf{a}_0 in the undeformed state and a rotation matrix,

$$\mathbf{a} = \mathbf{Q}\mathbf{a}_0. \quad (6.3)$$

In an incremental displacement formulation equation (6.2) must be linearized:

$$\Delta\mathbf{u} = \Delta\mathbf{r} + \Delta\mathbf{Q}\mathbf{a}_0, \quad (6.4)$$

where the linearization of the rotation matrix can be expressed in a more convenient form,

$$\Delta\mathbf{Q} = \hat{\mathbf{a}}\Delta\boldsymbol{\theta}. \quad (6.5)$$

Here is $\Delta\boldsymbol{\theta}^T = \Delta\theta_1, \Delta\theta_2, \Delta\theta_3$ and the matrix $\hat{\mathbf{a}}$ is

$$\hat{\mathbf{a}} = \begin{bmatrix} 0 & a_3 & -a_2 \\ -a_3 & 0 & a_1 \\ a_2 & -a_1 & 0 \end{bmatrix}. \quad (6.6)$$

For a model containing both deformable and rigid nodes the nodal degrees of freedom may be grouped, and the above expressions used to obtain a condensed set of unknowns:

$$\begin{Bmatrix} \Delta\mathbf{u}^D \\ \Delta\mathbf{u}^R \end{Bmatrix} = \begin{bmatrix} \mathbf{I} & \mathbf{0} & \mathbf{0} \\ \mathbf{0} & \mathbf{I} & \hat{\mathbf{a}} \end{bmatrix} \begin{Bmatrix} \Delta\mathbf{u}^D \\ \Delta\mathbf{r} \\ \Delta\boldsymbol{\theta} \end{Bmatrix} = \mathbf{A}\Delta\tilde{\mathbf{u}}. \quad (6.7)$$

Substituting this into the discrete form of the principle of virtual work yields expressions for the condensed finite element stiffness matrix and residual vector for the coupled rigid-deformable system:

$$\tilde{\mathbf{K}}\Delta\tilde{\mathbf{u}} = -\tilde{\mathbf{R}}, \quad \tilde{\mathbf{K}} = \mathbf{A}^T\mathbf{K}\mathbf{A}, \quad \tilde{\mathbf{R}} = \mathbf{A}^T\mathbf{R}. \quad (6.8)$$

6.1.2. A single rigid body

The global system of equations can now be written as follows (for a single rigid body coupled to a deformable body),

$$\begin{bmatrix} \mathbf{K}^D & \mathbf{K}^{DR} \\ \mathbf{K}^{DR^T} & \mathbf{K}^R \end{bmatrix} \begin{Bmatrix} \Delta \mathbf{u}^D \\ \Delta \mathbf{r} \\ \Delta \boldsymbol{\theta} \end{Bmatrix} = - \begin{Bmatrix} \mathbf{R}^D \\ \mathbf{F}^R \\ \mathbf{M}^R \end{Bmatrix}. \quad (6.9)$$

Here \mathbf{F}^R is formed by adding all the residual vectors of all interface nodes that connect the deformable body to the rigid body,

$$\mathbf{F}^R = \sum_i \mathbf{R}_i^D, \quad (6.10)$$

where i sums over all interface nodes, and

$$\mathbf{M}^R = \sum_i \hat{\mathbf{a}}_i \mathbf{R}_i^D. \quad (6.11)$$

It is recognized that \mathbf{F}^R is simply the total residual force that is applied to the rigid body and \mathbf{M}^R is the total residual torque.

Constructing the stiffness matrix is accomplished in a similar manner. Assume n nodes per element, then the normal element stiffness matrix (in absence of rigid nodes) is given by,

$$\mathbf{k}^{(e)} = \begin{bmatrix} \mathbf{k}_{11} & \cdots & \mathbf{k}_{1n} \\ \vdots & \ddots & \vdots \\ \mathbf{k}_{n1} & \cdots & \mathbf{k}_{nn} \end{bmatrix}, \quad (6.12)$$

where \mathbf{k}_{ij} is the nodal stiffness matrix connecting node i to node j . These nodal stiffness matrices are now assembled into the global stiffness matrix. If node i and j are neither interface nodes their nodal stiffness matrix is assembled into \mathbf{K}^D in the usual manner,

$$\mathbf{K}^D = \sum_e \mathbf{k}_{ij}^{(e)}, \quad (6.13)$$

where the sum now has to interpreted as the finite element assembly operator.

If node j is an interface node, than the nodal stiffness matrix gets assembled in the \mathbf{K}^{DR} matrix:

$$\mathbf{K}^{DR} = \sum_e \begin{bmatrix} \mathbf{k}_{ij}^{(e)} & \mathbf{k}_{ij}^{(e)} \hat{\mathbf{a}}_j \end{bmatrix}. \quad (6.14)$$

If both nodes belong to the rigid body than the nodal element matrix gets assembled in \mathbf{K}^R as follows,

$$\mathbf{K}^R = \sum_e \begin{bmatrix} \mathbf{k}_{ij}^{(e)} & \mathbf{k}_{ij}^{(e)} \hat{\mathbf{a}}_j \\ \hat{\mathbf{a}}_i^T \mathbf{k}_{ij}^{(e)} & \hat{\mathbf{a}}_i^T \mathbf{k}_{ij}^{(e)} \hat{\mathbf{a}}_j \end{bmatrix}. \quad (6.15)$$

6.1.3. Multiple Rigid Bodies

The previous results can easily be extended if there are multiple rigid bodies. The following section presents the approach for two rigid bodies, but the results can easily be generalized to N rigid bodies.

For two rigid bodies, the global system of equations takes the following form,

$$\begin{bmatrix} \mathbf{K}^D & \mathbf{K}_1^{DR} & \mathbf{K}_2^{DR} \\ \mathbf{K}_1^{DR\ T} & \mathbf{K}_{11}^R & \mathbf{K}_{12}^R \\ \mathbf{K}_2^{DR\ T} & \mathbf{K}_{21}^R & \mathbf{K}_{22}^R \end{bmatrix} \begin{Bmatrix} \Delta \mathbf{u}^D \\ \Delta \mathbf{r}_1 \\ \Delta \boldsymbol{\theta}_1 \\ \Delta \mathbf{r}_2 \\ \Delta \boldsymbol{\theta}_2 \end{Bmatrix} = - \begin{Bmatrix} \mathbf{R}^R \\ \mathbf{F}_1 \\ \mathbf{M}_1 \\ \mathbf{F}_2 \\ \mathbf{M}_2 \end{Bmatrix}. \quad (6.16)$$

Care must be taken to assemble the nodal stiffness matrix in the correct global sub-matrix. If node i is not an interface node and node j is connected to rigid body 1, then their nodal stiffness matrix goes into \mathbf{K}_1^{DR} . If, however, node j is attached to rigid body 2 then their nodal stiffness matrix goes into \mathbf{K}_2^{DR} . If node i is connected to rigid body 1 and node j is connected to rigid body 2, then their nodal stiffness matrix goes into \mathbf{K}_{12}^R , and so on. Note that it is assumed here that a node may only connect to a single rigid body.

6.2. Rigid Joints

A rigid joint is a location in space where two rigid bodies connect. The joint enforces a constraint on the system. This constraint can be written as,

$$\mathbf{c} \cdot \mathbf{Y}^c = \varphi^1 \cdot \mathbf{Y}^c - \varphi^2 \cdot \mathbf{Y}^c = 0 \quad (6.17)$$

Here \mathbf{Y}^c is the location of the joint in the reference configuration and φ^i $i=1,2$ is the deformation map of rigid body i . Equation (6.17) is a constraint equation that will be added to the total balance of virtual work.

$$G_{\varphi, w} = \sum_{i=1}^2 G^{\text{int, ext}}_{\varphi^i, w^i} - \underbrace{\sum_{i=1}^2 w^i \mathbf{Y}^c \cdot \mathbf{T}^i}_{G^c} = 0 \quad (6.18)$$

Here, the \mathbf{T}^i 's are the forces that will prevent the rigid bodies to separate at the joint position and $w^i = \delta \varphi^i$. First we note that due to the third law of Newton $\mathbf{T}^1 = -\mathbf{T}^2$, so that we can write the constraint term as,

$$G^c_{\varphi, w} = -\mathbf{T}^1 \cdot w^1 - w^2 \cdot \mathbf{Y}^c \quad (6.19)$$

Note that we can also write this as,

$$G^c_{\varphi, w} = -\mathbf{T}^1 \cdot \delta \mathbf{c} \quad (6.20)$$

The constraint forces are determined by the augmented Lagrangian method and are given by,

$$\mathbf{T} = \boldsymbol{\lambda} + \varepsilon_c \mathbf{c} \quad (6.21)$$

where $\boldsymbol{\lambda}$ is the Lagrange multiplier and ε_c is a user defined penalty factor.

The linearization of (6.20) is given by,

$$\begin{aligned} \Delta G^c_{\varphi, w} &= -\Delta \varepsilon_c \mathbf{c} \cdot \delta \mathbf{c} \\ &= -\varepsilon_c \Delta \mathbf{c} \cdot \delta \mathbf{c} \end{aligned} \quad (6.22)$$

Using the rigid body assumption, the quantity $\Delta \mathbf{c}$ can be written as follows,

$$\begin{aligned} \Delta \mathbf{c} &= \Delta \varphi^1 \mathbf{Y}^c - \Delta \varphi^2 \mathbf{Y}^c \\ &= \Delta \mathbf{r}_1 + \hat{\mathbf{y}}_1^c \Delta \boldsymbol{\theta}_1 - \Delta \mathbf{r}_2 - \hat{\mathbf{y}}_2^c \Delta \boldsymbol{\theta}_2 \end{aligned} \quad (6.23)$$

And similarly for $\delta \mathbf{c}$. If we now introduce the vectors,

$$\delta \Phi = \begin{bmatrix} \delta \mathbf{r}_1 \\ \delta \boldsymbol{\theta}_1 \\ \delta \mathbf{r}_2 \\ \delta \boldsymbol{\theta}_2 \end{bmatrix} \quad \mathbf{N} = \begin{bmatrix} \mathbf{T} \\ \hat{\mathbf{y}}_1^T \mathbf{T} \\ -\mathbf{T} \\ -\hat{\mathbf{y}}_2^T \mathbf{T} \end{bmatrix} \quad (6.24)$$

Then we can write the constraint work as,

$$G^c = -\delta \Phi^T \mathbf{N} \quad (6.25)$$

And the stiffness contribution as,

$$\Delta G^c = -\delta \Phi^T \mathbf{K}^c \Delta \Phi \quad (6.26)$$

$$\mathbf{K}^c = \varepsilon_c \begin{bmatrix} \mathbf{I} & \hat{\mathbf{y}}_1 & -\mathbf{I} & -\hat{\mathbf{y}}_2 \\ \hat{\mathbf{y}}_1^T & \hat{\mathbf{y}}_1^T \mathbf{y}_1 & -\mathbf{y}_1^T & -\mathbf{y}_1^T \mathbf{y}_2 \\ -\mathbf{I} & -\mathbf{y}_1 & \mathbf{I} & \mathbf{y}_2 \\ -\mathbf{y}_2^T & -\mathbf{y}_2^T \mathbf{y}_1 & \mathbf{y}_2^T & \mathbf{y}_2^T \mathbf{y}_2 \end{bmatrix} \quad (6.27)$$

6.3. Sliding Interfaces

This section summarizes the theoretical developments of the two body contact problem. After introducing some notation and terminology, the contact integral is presented, which contains the contribution to the virtual work equation from the contact tractions. Since the

nonlinear contact problem is solved using a Newton based iterative method, the contact integral is linearized. Next, anticipating a finite element implementation, the contact integral and its linearization are discretized using a standard finite element approach. Finally the augmented Lagrangian method for enforcing the contact constraints is described.

6.3.1. Contact Kinematics

For the most part the notation of this section follows [22], with a few simplifications here and there since the implementation in FEBio is currently for quasi-static, frictionless, two body contact problem.

The volume occupied by body i in the reference configuration is denoted by $\Omega^i \subset \mathbb{R}^3$ where $i=1,2$. The boundary of body i is denoted by Γ^i and is divided into three regions $\Gamma^i = \Gamma_\sigma^i \cup \Gamma_u^i \cup \Gamma_c^i$, where Γ_σ^i is the boundary where tractions are applied, Γ_u^i the boundary where the solution is prescribed and Γ_c^i the part of the boundary that will be in contact with the other body. It is assumed that $\Gamma_\sigma^i \cap \Gamma_u^i \cap \Gamma_c^i = \emptyset$.

The deformation of body i is defined by φ^i . The boundary of the deformed body i , that is the boundary of $\varphi^i \Omega^i$ is denoted by $\gamma^i = \gamma_\sigma^i \cup \gamma_u^i \cup \gamma_c^i$ where $\gamma_\sigma^i = \varphi^i \Gamma_\sigma^i$ is the boundary in the current configuration where the tractions are applied and similar definitions for γ_u^i and γ_c^i . See the figure below for a graphical illustration of the defined regions.

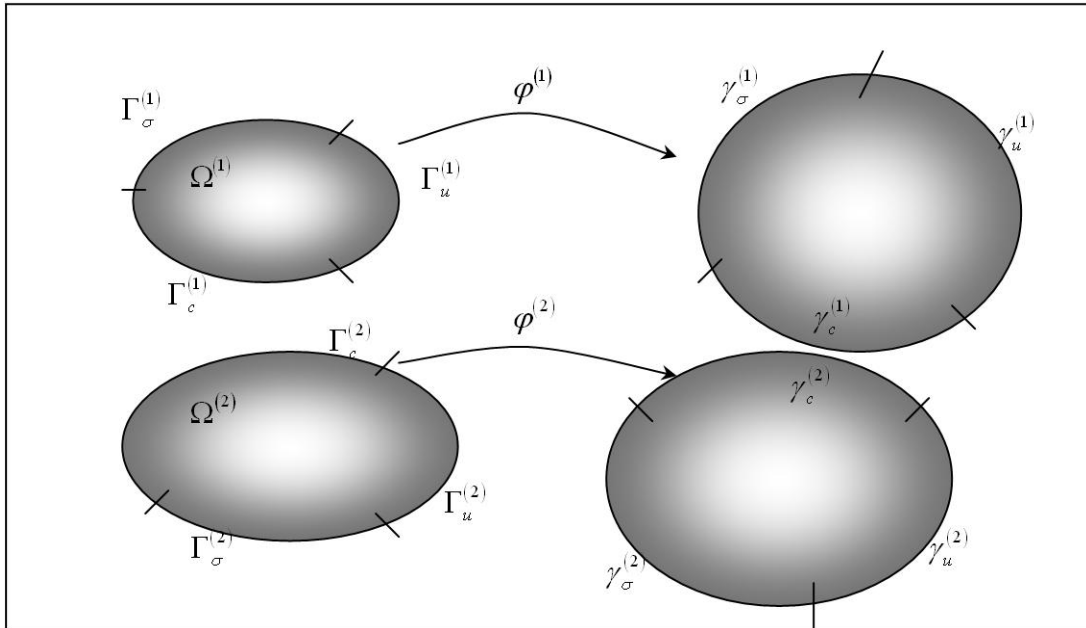


Figure 6-1. The two-body contact problem.

Points in body 1 are denoted by \mathbf{X} in the reference configuration and \mathbf{x} in the current configuration. For body 2 these points are denoted by \mathbf{Y} and \mathbf{y} . To define contact, the location where the two bodies are in contact with each other must be established. If body 1 is the *slave body* and body 2 is the *master body*, then for a given point \mathbf{X} on the slave reference contact surface there is a point $\bar{\mathbf{Y}}(\mathbf{X})$ on the master contact surface that is in some sense closest to point \mathbf{X} . This closest point is defined in a closest point projection sense:

$$\bar{\mathbf{Y}}(\mathbf{X}) = \arg \min_{\mathbf{Y} \in \Gamma_c^2} \left\| \varphi^1(\mathbf{X}) - \varphi^2(\mathbf{Y}) \right\|. \quad (6.28)$$

With the definition of $\bar{\mathbf{Y}}(\mathbf{X})$ established the *gap function* can be defined, which is a measure for the distance between \mathbf{X} and $\bar{\mathbf{Y}}(\mathbf{X})$,

$$g(\mathbf{X}) = -\mathbf{v} \cdot \left(\varphi^1(\mathbf{X}) - \varphi^2(\bar{\mathbf{Y}}(\mathbf{X})) \right), \quad (6.29)$$

where \mathbf{v} is the local surface normal of surface γ_c^2 evaluated at $\bar{\mathbf{y}} = \varphi^2(\bar{\mathbf{Y}}(\mathbf{X}))$. Note that $g > 0$ when \mathbf{X} has penetrated body 2, so that the constraint condition to be satisfied at all time is $g \leq 0$.

6.3.2. Weak Form of Two Body Contact

The balance of linear momentum can be written for each of the two bodies in the reference configuration,

$$\int_{\Omega^i} \text{GRAD}[w^i] : \mathbf{P}^i d\Omega - \int_{\Omega^i} w^i \cdot \mathbf{F}^i d\Omega - \int_{\Gamma_s^i} w^i \cdot \mathbf{T}^i d\Gamma - \int_{\Gamma_c^i} w^i \cdot \mathbf{T}^i d\Gamma = 0 \quad (6.30)$$

where w^i is a weighting function and \mathbf{P} is the 1st Piola-Kirchhoff stress tensor. The last term corresponds to the virtual work of the contact tractions on body i . For notational convenience, the notations φ and w are introduced to denote the collection of the respective mappings φ^i and w^i (for $i=1,2$). In other words,

$$\begin{aligned} \varphi : \bar{\Omega}^1 \cup \bar{\Omega}^2 &\rightarrow \mathbb{R}^3 \\ w : \bar{\Omega}^1 \cup \bar{\Omega}^2 &\rightarrow \mathbb{R}^3. \end{aligned} \quad (6.31)$$

The variational principle for the two body system is the sum of (6.30) for body 1 and 2 and can be expressed as,

$$\begin{aligned}
 G_{\varphi, w} &:= \sum_{i=1}^2 G^i_{\varphi^i, w^i} \\
 &= \sum_{i=1}^2 \left\{ \underbrace{\int_{\Omega^i} \text{GRAD}[w^i] : \mathbf{P}^i d\Omega - \int_{\Omega^i} w^i \cdot \mathbf{F}^i d\Omega - \int_{\Gamma_s^i} w^i \cdot \mathbf{T}^i d\Gamma}_{G^{\text{int}, \text{ext}}_{\varphi, w}} \right\} \quad (6.32) \\
 &\quad - \underbrace{\sum_{i=1}^2 \int_{\Gamma_c^i} w^i \cdot \mathbf{T}^i d\Gamma}_{G^c_{\varphi, w}}
 \end{aligned}$$

Or in short,

$$\boxed{G_{\varphi, w} = G^{\text{int}, \text{ext}}_{\varphi, w} + G^c_{\varphi, w}}. \quad (6.33)$$

Note that the minus sign is included in the definition of the contact integral G^c . The contact integral can be written as an integration over the contact surface of body 1 by balancing linear momentum across the contact surface:

$$\mathbf{t}^2 \cdot \bar{\mathbf{y}} \otimes \mathbf{x} d\Gamma^2 = -\mathbf{t}^1 \otimes \mathbf{x} d\Gamma^1. \quad (6.34)$$

The contact integral can now be rewritten over the contact surface of body 1:

$$G^c = - \int_{\Gamma_c^1} \mathbf{t}^1 \otimes \mathbf{x} \cdot \left[w^1 \otimes \mathbf{x} - w^2 \cdot \bar{\mathbf{y}} \otimes \mathbf{x} \right] d\Gamma. \quad (6.35)$$

In the case of frictionless contact, the contact traction is taken as perpendicular to surface 2 and therefore can be written as, $\mathbf{t}^1 = t_N \mathbf{v}$ where \mathbf{v} is the (outward) surface normal and t_N is to be determined from the solution strategy. For example in a Lagrange multiplier method the t_N 's would be the Lagrange multipliers.

By noting that the variation of the gap function is given by

$$\delta g = -\mathbf{v} \cdot \left[w^1 \otimes \mathbf{x} - w^2 \cdot \bar{\mathbf{y}} \otimes \mathbf{x} \right], \quad (6.36)$$

equation (6.35) can be simplified as,

$$\boxed{G^c = \int_{\Gamma_c^1} t_N \delta g d\Gamma}. \quad (6.37)$$

6.3.3. Linearization of the Contact Integral

In a Newton-Raphson implementation the contact integral must be linearized with respect to the current configuration:

$$\Delta G^c_{\varphi, w} = \int_{\Gamma_c^1} \Delta t_N \delta g d\Gamma. \quad (6.38)$$

Examining the normal contact term first, the directional derivative of t_N is given (for the case of the penalty regularization) by:

$$\begin{aligned}\Delta t_N &= \Delta \varepsilon_N \langle g \rangle \\ &= H(g) \varepsilon_N \Delta g,\end{aligned}\quad (6.39)$$

where ε_N is the penalty factor and $H(g)$ is the Heaviside function. The quantity $\Delta \delta g$ is given by,

$$\begin{aligned}\Delta \delta g &= g \left[\mathbf{v} \cdot \delta \varphi_{,\gamma}^2 \bar{\mathbf{Y}} \mathbf{X} + \kappa_{\alpha\gamma} \bar{\mathbf{Y}} \mathbf{X} \delta \bar{\xi}_\alpha^\gamma \right] m^{\gamma\beta} \\ &\quad \left[\mathbf{v} \cdot \Delta \varphi_{,\beta}^2 \bar{\mathbf{Y}} \mathbf{X} + \kappa_{\alpha\beta} \bar{\mathbf{Y}} \mathbf{X} \Delta \bar{\xi}^\alpha \right] \\ &\quad + \delta \bar{\xi}^\beta \mathbf{v} \cdot \left[\Delta \varphi_{,\beta}^2 \bar{\mathbf{Y}} \mathbf{X} \right] + \Delta \bar{\xi}^\beta \mathbf{v} \cdot \left[\delta \varphi_{,\beta}^2 \bar{\mathbf{Y}} \mathbf{X} \right] \\ &\quad + \kappa_{\alpha\beta} \bar{\mathbf{Y}} \mathbf{X} \delta \bar{\xi}^\beta \Delta \bar{\xi}^\alpha\end{aligned}\quad (6.40)$$

6.3.4. Discretization of the Contact Integral

The contact integral, which is repeated here,

$$G^c(\varphi, w) = \int_{\Gamma^1} t_N \delta g d\Gamma, \quad (6.41)$$

will now be discretized using a standard finite element procedure. First it is noted that the integration can be written as a sum over the surface element areas:

$$G^c(\varphi, w) = \sum_{e=1}^{N_{sel}} \int_{\Gamma^{1e}} t_N \delta g d\Gamma, \quad (6.42)$$

where N_{sel} is the number of surface elements. The integration can be approximated using a quadrature rule,

$$G^c(\varphi, w) \cong \sum_{e=1}^{N_{sel}} \left\{ \sum_{i=1}^{N_{int}^e} w^i j_{\xi_i} t_N \xi_i \delta g \xi_i \right\}, \quad (6.43)$$

where N_{int}^e are the number of integration points for element e . It is now assumed that the integration points coincide with the element's nodes (e.g. for a quadrilateral surface element we have $\xi_1 = -1, -1$, $\xi_2 = 1, -1$, $\xi_3 = 1, 1$ and $\xi_4 = -1, 1$). With this quadrature rule, we have

$$\begin{aligned}w^1 \xi_i &= \mathbf{c}_i^1 \\ w^2 \bar{\xi}_i &= \sum_{j=1}^n N_j^2 \bar{\xi}_i \mathbf{c}_j^2,\end{aligned}\quad (6.44)$$

so that,

$$\delta g \xi_i = -\mathbf{v} \cdot \left(\mathbf{c}_i^1 - \sum_{j=1}^n N_j^2 \bar{\xi}_i \mathbf{c}_j^2 \right). \quad (6.45)$$

If the following vectors are defined,

$$\begin{aligned}\delta \Phi^T &= [\mathbf{c}_i^1, \mathbf{c}_1^2, \dots, \mathbf{c}_n^2] \\ \mathbf{N}^T &= [\mathbf{v}, -\mathbf{v} N_1^2, \dots, -\mathbf{v} N_n^2]\end{aligned}\quad (6.46)$$

equation (6.43) can then be rewritten as follows,

$$G^c \varphi, \delta \mathbf{v} \cong \sum_{e=1}^{N_{sel}} \left\{ \sum_{i=1}^{N_{int}^e} w_i j \xi_i t_N \xi_i \delta \Phi^T \mathbf{N}^T \right\}. \quad (6.47)$$

The specific form for t_N will depend on the method employed for enforcing the contact constraint.

6.3.5. Discretization of the Contact Stiffness

A similar procedure can now be used to calculate the discretized contact stiffness matrix. The linearization of the contact integral is repeated here:

$$\begin{aligned} \Delta G^c \varphi, w &= \sum_{e=1}^{N_{sel}} \int_{\Gamma^e} \Delta t_N \delta g \, d\Gamma \\ &= \sum_{e=1}^{N_{sel}} \sum_{i=1}^{N_{int}^e} w_i j \xi_i \Delta t_N \delta g \xi_i \end{aligned} \quad (6.48)$$

Using matrix notation we can rewrite equation (6.48) as,

$$\Delta W^c \varphi, \delta \mathbf{v} = \sum_{e=1}^{N_{sel}} \sum_{i=1}^{N_{int}^e} w_i j \xi_i \delta \Phi \cdot \mathbf{k}^c \Delta \Phi, \quad (6.49)$$

where $\delta \Phi$ is as above and $\Delta \Phi$ similar to $\delta \Phi$ with δ replaced with Δ and \mathbf{k}^c ,

$$\begin{aligned} \mathbf{k}^c &= \varepsilon_N H \lambda_N^k + \varepsilon_N g \mathbf{N} \mathbf{N}^T + t_N g \left[m^{11} \bar{\mathbf{N}}_1 \bar{\mathbf{N}}_1^T \right. \\ &\quad \left. + m^{12} \bar{\mathbf{N}}_1 \bar{\mathbf{N}}_2^T + \bar{\mathbf{N}}_2 \bar{\mathbf{N}}_1^T + m^{22} \bar{\mathbf{N}}_2 \bar{\mathbf{N}}_2^T \right] - \mathbf{D}_1 \mathbf{N}_1^T \\ &\quad - \mathbf{D}_2 \mathbf{N}_2^T - \mathbf{N}_1 \mathbf{D}_1^T - \mathbf{N}_2 \mathbf{D}_2^T + \kappa_{12} \mathbf{D}_1 \mathbf{D}_2^T + \mathbf{D}_2 \mathbf{D}_1^T \end{aligned} \quad (6.50)$$

where,

$$\mathbf{N} = \begin{bmatrix} \mathbf{v} \\ -N_1 \bar{\xi} \mathbf{v} \\ \vdots \\ -N_4 \bar{\xi} \mathbf{v} \end{bmatrix}, \quad \mathbf{T}_\alpha = \begin{bmatrix} \boldsymbol{\tau}_\alpha \\ -N_1 \bar{\xi} \boldsymbol{\tau}_\alpha \\ \vdots \\ -N_4 \bar{\xi} \boldsymbol{\tau}_\alpha \end{bmatrix}, \quad \mathbf{N}_\alpha = \begin{bmatrix} \mathbf{0} \\ -N_{1,\alpha} \bar{\xi} \mathbf{v} \\ \vdots \\ -N_{4,\alpha} \bar{\xi} \mathbf{v} \end{bmatrix}. \quad (6.51)$$

The following vectors are also defined which depend on the vectors of (6.51):

$$\begin{aligned} \mathbf{D}_1 &= \frac{1}{\det \mathbf{A}} \begin{bmatrix} A_{22} \mathbf{T}_1 + g \mathbf{N}_1 & -A_{12} \mathbf{T}_2 + g \mathbf{N}_2 \end{bmatrix} \\ \mathbf{D}_2 &= \frac{1}{\det \mathbf{A}} \begin{bmatrix} A_{11} \mathbf{T}_2 + g \mathbf{N}_2 & -A_{12} \mathbf{T}_1 + g \mathbf{N}_1 \end{bmatrix}, \\ \bar{\mathbf{N}}_1 &= \mathbf{N}_1 - \kappa_{12} \mathbf{D}_2 \\ \bar{\mathbf{N}}_2 &= \mathbf{N}_2 - \kappa_{12} \mathbf{D}_1 \end{aligned} \quad (6.52)$$

where the matrix \mathbf{A} is defined as,

$$A_{ij} = m_{ij} + g \kappa_{ij}. \quad (6.53)$$

Here, $m_{ij} = \mathbf{\tau}_i \cdot \mathbf{\tau}_j$ is the surface metric tensor and $\kappa_{ij} = \mathbf{v} \cdot \varphi_{t,ij}^2$ $\bar{\mathbf{Y}}$ denotes the components of the surface curvature at $\bar{\xi}$.

6.3.6. Augmented Lagrangian Method

The augmented Lagrangian method is used in FEBio to enforce the contact constraints to a user-specified tolerance. This implies that the normal contact tractions are given by,

$$\mathbf{t}_N = \langle \lambda_N + \varepsilon_N g \rangle. \quad (6.54)$$

Note that this assumption is consistent with the approach that was used in establishing the discretization of the linearization of the contact integral (6.50). In (6.54) ε_N is a penalty factor that is chosen arbitrarily.

The Newton-Raphson iterative method is now used to solve the nonlinear contact problem where Uzawa's method (REF) is employed to calculate the Lagrange multipliers λ_N . This implies that the Lagrange multipliers are kept fixed during the Newton-Raphson iterations. After convergence the multipliers are updated and a new NR procedure is started. This procedure can be summarized by the following four steps.

1. **Initialize** the augmented Lagrangian iteration counter k , and the initial guesses for the multipliers:

$$\begin{aligned} \lambda_{N_{n+1}}^0 &= \lambda_{N_n} \\ k &= 0 \end{aligned} \quad (6.55)$$

2. **Solve** for \mathbf{d}_{n+1}^k , the solution vector corresponding to the fixed k th iterate for the multipliers,

$$\mathbf{F}^{\text{int}} \mathbf{d}_{n+1}^k + \mathbf{F}^c \mathbf{d}_{n+1}^k = \mathbf{F}_{n+1}^{\text{ext}}, \quad (6.56)$$

where the contact tractions used to compute \mathbf{F}^c , the contact force, are governed by

$$\mathbf{t}_{N_{n+1}}^k = \langle \lambda_{N_{n+1}}^k + \varepsilon_N g_{n+1}^k \rangle. \quad (6.57)$$

3. **Update** the Lagrange multipliers and iteration counters:

$$\begin{aligned} \lambda_{N_{n+1}}^{k+1} &= \langle \lambda_{N_{n+1}}^k + \varepsilon_N g_{n+1}^k \rangle \\ k &= k + 1 \end{aligned} \quad (6.58)$$

4. **Return** to the solution phase.

Steps 2-4 of the above algorithm are generally repeated until all contact constraints are satisfied to a user-specified tolerance or little change in the solution vector from augmentation to augmentation is noted.

6.3.7. Automatic penalty calculation

The determination of the penalty factor ε_N can be a difficult task, since a good value may depend on both material parameters and geometrical factors. In FEBio the value of this penalty factor can be determined automatically. In this case FEBio will calculate a penalty factor for each facet using the following formula.

$$\varepsilon_i = \frac{f_{sl} K_i A_i^2}{V_i} \quad (6.59)$$

Here, K_i is the effective bulk modulus, A_i the surface area of the facet, V_i the volume of the element to which this facet belongs and f_{sl} a user defined scale factor.

6.3.8. Alternative formulations

As of FEBio version 1.2, two alternative formulations for sliding contact are available. The first method, which is referred to as the *facet-to-facet sliding*, is very similar to the formulation described above. It only differs in that it uses a Gaussian quadrature rule instead of nodal integration. Because of the more accurate integration rule, it was noted that this method in many situations was more stable and resulted in better convergence.

The second alternative differs more significantly from the method described above. It also begins with the definition of a single contact integral over the slave surface.

$$G_c = - \int_{\gamma^1} \mathbf{t}_c \cdot \delta \varphi^1 - \delta \bar{\varphi}^2 \, da \quad (6.60)$$

But a different derivation is followed to obtain the linearization of this contact integral. The main reason for this difference is a subtly alternative definition for the gap function. In this method, it is defined as follows.

$$g(\mathbf{X}) = \mathbf{v}^1 \cdot \varphi^1(\mathbf{X}) - \bar{\varphi}^2(\bar{\mathbf{Y}}(\mathbf{X})) \quad (6.61)$$

where, \mathbf{v}^1 is the normal of the slave surface (opposed to the master normal as used in the derivation above). In this case, the point $\bar{\mathbf{Y}}(\mathbf{X})$ is no longer the closest point projection of \mathbf{X} onto the master surface, but instead is the normal projection along \mathbf{v}^1 . The linearization of equation (6.61) now becomes,

$$\delta g = \mathbf{v}^1 \cdot \delta \varphi^1(\mathbf{X}) - \delta \bar{\varphi}^2(\bar{\mathbf{Y}}(\mathbf{X})) - \boldsymbol{\tau}_i^2 \delta \xi_i \quad (6.62)$$

Where, $\boldsymbol{\tau}_i^2 = \frac{\partial \bar{\varphi}^2}{\partial \eta_i}$ are the tangent vectors to the master surface at $\bar{\mathbf{Y}}(\mathbf{X})$. Note that

since \mathbf{v}^1 is normal to the slave surface, equation (6.62) does not reduce to equation (6.36).

In one assumes frictionless contact, the contact traction can be written as follows,

$$\mathbf{t}_c = t_n \mathbf{v}^1 = t_n \frac{\boldsymbol{\tau}_1^1 \times \boldsymbol{\tau}_2^1}{\|\boldsymbol{\tau}_1^1 \times \boldsymbol{\tau}_2^1\|} \quad (6.63)$$

where, $\boldsymbol{\tau}_i^1$ are the tangent vectors to γ^1 evaluated at \mathbf{X} . Using (6.63) we can rewrite the contact integral as follows.

$$G_c = - \int_{\xi^1} t_n \delta\varphi^1 - \delta\bar{\varphi}^2 \cdot \boldsymbol{\tau}_1^1 \times \boldsymbol{\tau}_2^1 d\xi \quad (6.64)$$

Where we assumed that the integration domain can be mapped to a 2D parametric domain, $\mathbf{x} = \mathbf{x}(\xi_\alpha)$.

The linearization of (6.64) now proceeds in the usual fashion. Omitting the details, it can be shown that the linearization of the contact integral results in,

$$\begin{aligned} DG_c = & \int_{\xi^1} \varepsilon \mathbf{v}^1 \cdot \mathbf{u}_2 - \mathbf{u}_1 + \bar{\boldsymbol{\tau}}_\alpha^2 \Delta \xi_2^\alpha \delta\varphi_1 - \delta\bar{\varphi}_2 \cdot \boldsymbol{\tau}_1^1 \times \boldsymbol{\tau}_2^1 d\xi \\ & - \int_{\xi^1} t_n \frac{\partial \mathbf{u}_1}{\partial \xi_\alpha} \left(\mathbf{u}_1 - \mathbf{u}_2 \cdot a^{\alpha\beta} \boldsymbol{\tau}_\beta^1 - a^{\alpha\beta} g \mathbf{v}^1 \cdot \frac{\partial \mathbf{u}_1}{\partial \xi_\beta} \right) d\xi \\ & + \int_{\xi^1} t_n \delta\varphi_1 - \delta\bar{\varphi}_2 \cdot \left(\frac{\partial \mathbf{u}_1}{\partial \xi_1} \times \boldsymbol{\tau}_2^1 + \boldsymbol{\tau}_1^1 \times \frac{\partial \mathbf{u}_1}{\partial \xi_2} \right) d\xi \end{aligned} \quad (6.65)$$

where, $a_{\alpha\beta} = \boldsymbol{\tau}_\alpha^1 \times \boldsymbol{\tau}_\beta^2$ and $a^{\alpha\beta} = a^{-1}_{\alpha\beta}$.

The discretization of the contact integral and its linearization now proceeds as usual. We will not derive the details, but it is important to point out that the resulting stiffness matrix for this particular contact formulation is not symmetric. Although this method has shown to give good results, especially in large compression problems, it was desirable to derive a symmetric version as well. Because of this, a slightly different formulation was also developed that does reduce to a symmetric stiffness matrix although this symmetric version did not seem to perform as well as the non-symmetric one.

6.4. Biphasic Contact

As of version 1.2 FEBio also provides a biphasic contact algorithm. This contact formulation allows fluid to flow across the contact interface. The implementation is based on the alternative contact formulation explained in section 6.3.8. In the case of biphasic contact an additional contact constraint needs to be enforced: The fluid flow across the contact interface must be the same. This can be expressed in a variational formulation as follows.

$$G_p = \int_{\gamma^1} q \delta p^1 - \delta \bar{p}^2 da = 0 \quad (6.66)$$

where q is a Lagrange multiplier that enforces the constraint. For example, using the penalty method, it can be given by,

$$q = \varepsilon_p (p^1 - \bar{p}^2) \quad (6.67)$$

where ε_p is a user defined parameter. Note that equation (6.66) is both a function of the unknown interface pressures as well as the unknown displacements due to the integration over the unknown domain γ^1 as well as due to the fact that \bar{p}^2 and $\delta\bar{p}^2$ need to be evaluated over the unknown surface γ^2 . The discretization and linearization of (6.66) now proceed in the usual fashion. Details are omitted but can be found in [23].

6.5. Tied Contact

In some situations it is useful to connect two non-conforming meshes together. This can be done by defining a tied contact interface. In FEBio, the tied contact works very similar to the sliding contact interface. We need to define a slave surface and a master surface, where it is assumed that the slave surface nodes will be tied to the master surface faces.

6.5.1. Gap Function

Just as in sliding contact, we need to define a gap function that measures the distance between the slave and master surface. In order to do that, we first define the projection of a slave node to the master surface.

$$\bar{\mathbf{Y}}(\mathbf{X}) = \arg \min_{\mathbf{Y} \in \Gamma^2} \|\mathbf{X} - \mathbf{Y}\| \quad (6.68)$$

This definition is similar to that of the sliding interface, except that now the projection is done in the material reference frame. This implies that the projection only needs to be calculated once, at the beginning of the analysis. We can now proceed to the definition of the gap function.

$$\mathbf{g}(\mathbf{X}) = \varphi^1(\mathbf{X}) - \varphi^2(\bar{\mathbf{Y}}(\mathbf{X})) \quad (6.69)$$

An important observation is that the gap function is now a vector quantity since the gap needs to be closed in all direction, not just the normal direction as is the case in sliding contact.

6.5.2. Tied Contact Integral

With the definition of the gap function at hand (equation (6.69)), we can define the contribution to the virtual work equation from the tied contact reaction forces.

$$W_t = \int_{\Gamma_c} \mathbf{T} \cdot \delta \mathbf{g} d\Gamma \quad (6.70)$$

Here, \mathbf{T} is the reaction force that enforces the constraint $\mathbf{g}(\mathbf{X}) = 0$. Since we anticipate the use of an augmented Lagrangian formalism, we can write this reaction force as follows.

$$\mathbf{T} = \lambda + \varepsilon \mathbf{g} \quad (6.71)$$

The vector quantity λ is the Lagrangian multiplier and ε is a penalty factor.

6.5.3. Linearization of the Contact Integral

Since equation (6.70) is nonlinear we need to calculate the linearization. For tied contact, this is simply given by the following equation.

$$\Delta W_t = \int_{\Gamma_c} \varepsilon \Delta \mathbf{g} \cdot \delta \mathbf{g} d\Gamma \quad (6.72)$$

Where

$$\delta \mathbf{g} = \mathbf{w}^1 - \mathbf{w}^2 \quad (6.73)$$

and

$$\Delta \mathbf{g} = \Delta \varphi^1 \mathbf{X} - \Delta \varphi^2 \bar{\mathbf{Y}} \mathbf{X} \quad (6.74)$$

We also introduced the notation $\mathbf{w}^i = \delta \varphi^i$.

The discretization of (6.72) will lead to a contribution to the stiffness matrix. Notice that due to symmetry between $\delta \mathbf{g}$ and $\Delta \mathbf{g}$ this matrix will be symmetric.

6.5.4. Discretization

The contact integral (6.70) can be discretized as follows. First, we split the integration over all the slave surface elements.

$$W_t = \sum_{e=1}^{nel} \int_{\Gamma_c^e} \mathbf{T} \cdot \delta \mathbf{g} d\Gamma^e \quad (6.75)$$

The integration can be approximated by a quadrature rule,

$$W_t = \sum_{e=1}^{nel} \sum_{i=1}^{N_{int}^e} w^i j_{\xi_i} \mathbf{T}_{\xi_i} \cdot \delta \mathbf{g}_{\xi_i} \quad (6.76)$$

If we use a nodally integrated elements, we have

$$\begin{aligned} \mathbf{w}^1_{\xi_i} &= \mathbf{c}_i^1 \\ \mathbf{w}^2_{\xi_i} &= \sum_j N_j \bar{\xi}_i \mathbf{c}_j^2 \end{aligned} \quad (6.77)$$

so that,

$$\delta \mathbf{g}_{\xi_i} = \mathbf{c}_i^1 - \sum_j N_j \bar{\xi}_i \mathbf{c}_j^2 \quad (6.78)$$

We can now write the contact integral (6.75) in its final form,

$$W_t = \sum_{e=1}^{nel} \sum_{i=1}^{N_{int}^e} w^i j_{\xi_i} \mathbf{N}_{\xi_i} \mathbf{T}_{\xi_i} \cdot \delta \Phi \quad (6.79)$$

where

$$\delta \Phi^T \xi_i = \left[\mathbf{c}_i^1, \mathbf{c}_1^2, \mathbf{c}_2^2, \dots, \mathbf{c}_n^2 \right] \quad (6.80)$$

$$\mathbf{N} \xi_i = \mathbf{I}, -\mathbf{N}_1, \dots, -\mathbf{N}_n \quad (6.81)$$

and

$$\mathbf{N}_i = \begin{bmatrix} N_i & 0 & 0 \\ 0 & N_i & 0 \\ 0 & 0 & N_i \end{bmatrix} \quad (6.82)$$

For the linearized tied contact integral (6.72), a similar discretization procedure leads to,

$$\Delta W_t = \sum_{e=1}^{nel} \sum_{i=1}^{N_{\text{un}}^e} w^i j \xi_i \Delta \Phi \cdot \mathbf{K}_c \delta \Phi \quad (6.83)$$

where

$$\mathbf{K}_c = \varepsilon \mathbf{N}^T \mathbf{N} \quad (6.84)$$

References

1. Bonet, J. and R.D. Wood, *Nonlinear continuum mechanics for finite element analysis*. 1997: Cambridge University Press.
2. Spencer, A.J.M., *Continuum Theory of the Mechanics of Fibre-Reinforced Composites*. 1984, New York: Springer-Verlag.
3. Weiss, J.A., B.N. Maker, and S. Govindjee, *Finite element implementation of incompressible, transversely isotropic hyperelasticity*. *Computer Methods in Applications of Mechanics and Engineering*, 1996. **135**: p. 107-128.
4. Horowitz, A., et al., *Nonlinear Incompressible Finite Element for Simulating Loading of Cardiac Tissue- part I: two Dimensional Formulation for Thin Myocardial Strips*. *Journal of Biomechanical Engineering, Transactions of the ASME*, 1988. **110**(1): p. 57-61.
5. Humphrey, J.D., R.K. Strumpf, and F.C.P. Yin, *Determination of a constitutive relation for passive myocardium. I. A new functional form*. *Journal of Biomechanical Engineering, Transactions of the ASME*, 1990. **112**(3): p. 333-339.
6. Humphrey, J.D. and F.C.P. Yin, *On constitutive Relations and Finite Deformations of Passive Cardiac Tissue: I. A Pseudostrain-Energy Function*. *Journal of Biomechanical Engineering, Transactions of the ASME*, 1987. **109**(4): p. 298-304.
7. Matthies, H. and G. Strang, *The solution of nonlinear finite element equations*. *Intl J Num Meth Eng*, 1979. **14**: p. 1613-26.
8. Simo, J.C. and R.L. Taylor, *Quasi-incompressible finite elasticity in principal stretches: Continuum basis and numerical algorithms*. *Computer Methods in Applied Mechanics and Engineering*, 1991. **85**: p. 273-310.
9. Hughes, J.R. and W.K. Liu, *Nonlinear Finite Element Analysis of Shells: Part I. Three-dimensional Shells*. *Computer Methods in Applied Mechanics and Engineering*, 1980. **26**: p. 331-362.
10. Betsch, P., F. Gruttmann, and S. E., *A 4-node finite shell element for the implementation of general hyperelastic 3D-elasticity at finite strains*. *Comput. Methods Appl. Mech. Engrg*, 1996. **130**: p. 57-79.
11. Veronda, D.R. and R.A. Westmann, *Mechanical Characterization of Skin - Finite Deformations*. *J. Biomechanics*, 1970. **Vol. 3**: p. 111-124.
12. Puso, M.A. and J.A. Weiss, *Finite element implementation of anisotropic quasi-linear viscoelasticity using a discrete spectrum approximation*. *J Biomech Eng*, 1998. **120**(1): p. 62-70.
13. Quapp, K.M. and J.A. Weiss, *Material characterization of human medial collateral ligament*. *J Biomech Eng*, 1998. **120**(6): p. 757-63.
14. Bowen, R.M., *Incompressible porous media models by use of the theory of mixtures*. *Int J Eng Sci*, 1980. **18**(9): p. 1129-1148.
15. Mow, V.C., et al., *Biphasic creep and stress relaxation of articular cartilage in compression: Theory and experiments*. *J. Biomech. Eng.*, 1980. **102**: p. 73-84.
16. Truesdell, C. and R. Toupin, *The classical field theories*. *Handbuch der physik*, ed. S. Flugge. Vol. III/1. 1960, Heidelberg: Springer.

17. Un, K. and R.L. Spilker, *A penetration-based finite element method for hyperelastic 3D biphasic tissues in contact. Part II: finite element simulations*. J Biomech Eng, 2006. **128**(6): p. 934-42.
18. Curnier, A., H. Qi-Chang, and P. Zysset, *Conewise linear elastic materials*. J Elasticity, 1994. **37**(1): p. 1-38.
19. Ateshian, G.A., B.J. Ellis, and J.A. Weiss, *Equivalence between short-time biphasic and incompressible elastic material responses*. J Biomech Eng, 2007. **129**(3): p. 405-12.
20. Guccione, J.M. and A.D. McCulloch, *Mechanics of active contraction in cardiac muscle: part I - constitutive relations for fiber stress that describe deactivation*. J. Biomechanical Engineering, 1993. **vol. 115**(no. 1): p. 72-83.
21. Maker, B.N., *Rigid bodies for metal forming analysis with NIKE3D*. University of California, Lawrence Livermore Lab Rept, 1995. **UCRL-JC-119862**: p. 1-8.
22. Laursen, T.A., *Computational Contact and Impact Mechanics*. 2002: Springer.
23. Ateshian, G., S. Maas, and J.A. Weiss, *Finite element algorithm for frictionless contact of porous permeable media under finite deformation and sliding*. J. Biomech. Engn., 2010. **132**(6): p. 1006-1019.